TASK FORCE REPORT

DOT-105/111/112/114 TANK CARS SHELL CRACKING AND STRUCTURAL INTEGRITY ASSESSMENT

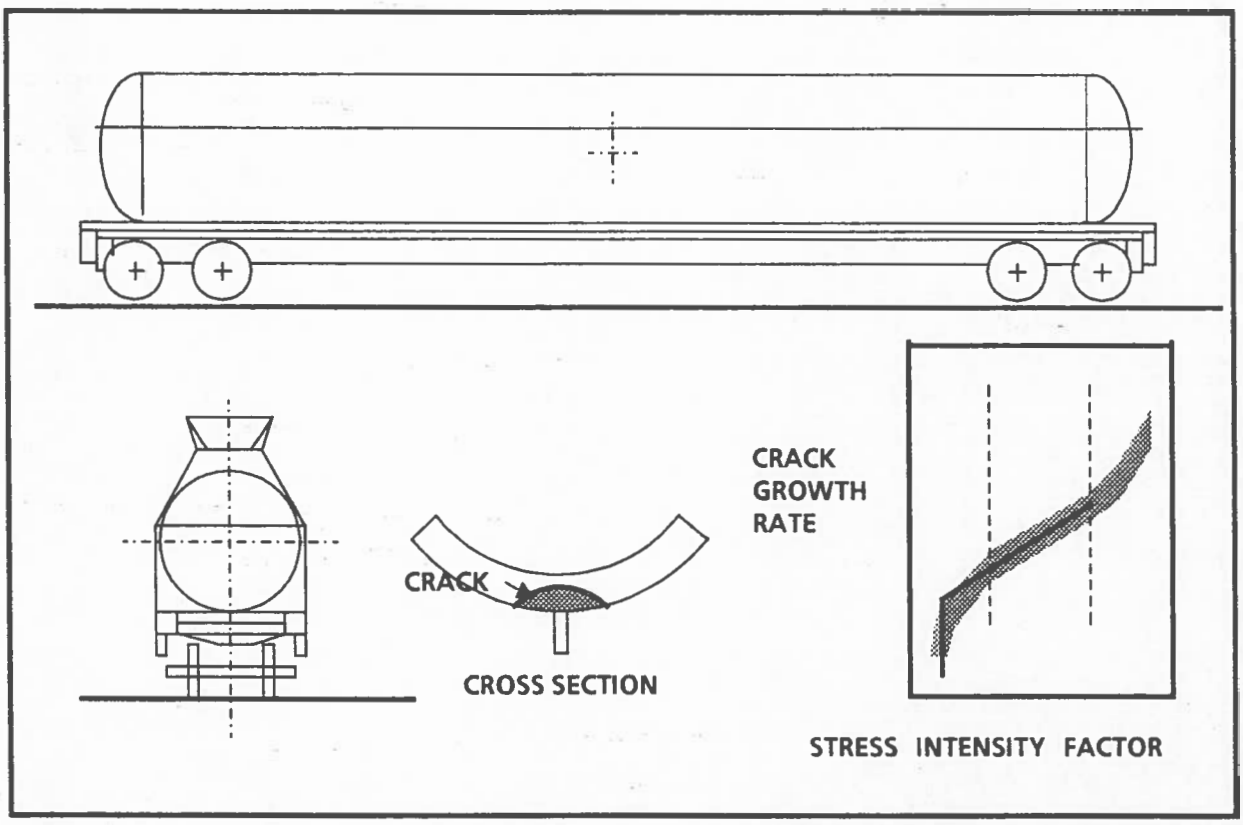

DOT TRANSPORTATION SYSTEMS CENTER
Cambridge, MA 02142
February 1986

TABLE OF CONTENTS

LIST OF FIGURES

LIST OF TABLES

Executive Summary

The discovery and investigation of a tank car leaking ethylene oxide on December 31, 1984, at North Little Rock, Arkansas, revealed that the subject car had been equipped with an anti-shift bracket not in conformance with federal regulations for such brackets on tank cars carrying hazardous materials. (The function of the anti-shift bracket is to restrain the outer insulating shell against motion relative to the tank shell.) The Federal Railroad Administration (FRA) Office of Safety subsequently reviewed construction records and had identified, by September 1985, approximately 9,000 hazardous material cars with non-conforming brackets. These cars were built by one manufacturer, who proposed to bring the affected cars into conformance by means of a campaign to remove the non-conforming brackets, inspect the tank shell for cracks, and remove or repair any detected cracks before returning the car to service. The manufacturer immediately started the campaign and, by August 1985, had inspected approximately 3,000 cars, of which some 200 were found to have cracks similar to the original crack discovered at North Little Rock. By mid-December 1985, over 7,400 cars had been inspected.

The 9,000 affected cars represent over 10 percent of the nation's capacity for carrying hazardous materials by rail and nearly $700 million in capital investment at current prices for new construction. There is thus a strong and legitimate incentive to return the affected cars to service as quickly as possible. On the other hand, many of the commodities carried in these cars are highly toxic and/or flammable. It is thus also essential to assure that the cars can be returned to service without substantially increasing public safety and health risks.

In August 1985, the FRA Associate Administrator for Safety asked the DOT Transportation Systems Center to make a preliminary technical assessment of the adequacy of the manufacturer's inspection and repair procedures. The Center formed a task force for this purpose, consisting of five senior engineering faculty members from three universities, a National Bureau of Standards expert on tank car steels, and two senior members of the Center's technical staff. The task force members are nationally recognized authorities on structures, structural fatigue, and fracture mechanics.

This report summarizes the task force assessment of the inspection and repair procedures. The task force has identified two major technical issues: adequacy of crack detection; and ability to repair detected cracks without collateral damage.

The manufacturer's approach to crack detection is a one-time check based on the dye penetrant method. The task force concludes that a single inspection has the risk of returning cars to service with undetected cracks, that such cracks can grow in the fatigue environment created by normal service loads, and that the level of risk is unacceptable for carriage of hazardous materials. The task force recommends that the manufacturer's inspection campaign be repeated at intervals, the length of the interval depending on the car wall thickness and commodity carried. The recommended inspection intervals are: 5,000 miles for cars with 7/16-inch walls carrying ethylene oxide; 15,000 miles for all other 7/16 wall cars; 205,000 miles for 9/16 wall cars, except as noted below; and one million miles for 11/16 wall cars. The repeated inspections establish a low level of risk in a manner similar to the current practice for risk assessment of flight-safety-critical structure in transport category airplanes certified for commercial service. The task force additionally recommends that 9/16 wall cars in the affected fleet be restricted from carrying propylene.

The task force further recommends that reinspection be performed on 100 percent of the cars that carry highly toxic and/or flammable materials, viz: all liquefied flammable gases, ethylene oxide, anhydrous ammonia, and other liquids that readily vaporize to create inhalation hazards. However, that part of the fleet which carries other hazardous materials that do not pose the same level of immediate safety threat (e.g., acids) can be adequately protected by examining a sample of 150 cars per

reinspection, with the understanding that a 100 percent inspection should be performed if the sample is found to contain a car with a crack.

The manufacturer's approach to repair closely follows the provisions for good welding practice, as established by the Association of American Railroads (AAR). The AAR standards are comparable to established practices in other industries. However, the task force notes that even the best of standards does not guarantee that every weld will be free of defects that might create collateral damage which could grow in fatigue. The recommended periodic reinspection can protect the fleet against potential failures from a small incidence of collateral damage, but risk of excessive incidence should not be tolerated. Therefore, the task force recommends that the post-weld stress relief and X-ray check procedures now performed on all pressure cars and some non-pressure cars be applied to all cars that are repaired by welding. The task force believes that any remaining incidence of welding damage will not pose any significant risk of tank shell failure. The task force recommends that this belief be documented by cross checking weld repair reports with accident reports to confirm that there is no correlation of shell failures with weld repairs.

1. Background

On December 31, 1984, a railroad employee in a North Little Rock, Arkansas, classification yard discovered an active leak in tank car RAIX 7033, shortly after the car had been humped. The car was later emptied, purged, and removed from service without further incident. The car was a DOT-111A/100W specification car carrying ethylene oxide, a toxic and flammable liquid.

The leak incident was subsequently investigated by the National Transportation Safety Board (Burnett et al., 1985). The Board's investigation revealed that the leak had occurred at a crack through the tank car shell. The crack had originated in the heat affected zone of a weld used to attach an anti-shift bracket to the shell and had apparently completed its propagation through the shell wall when the car was subjected to coupling loads after humping. Figure 1 illustrates the crack location and orientation.

The tank car was found to have reached a speed of 12 mph before decelerating and coupling to a consist of eight loaded grain hopper cars. The following car, a loaded box car, reached a speed of almost 14 mph before decelerating and coupling to the tank car. When a gravity hump is used to classify freight cars, the cars run through friction retarders immediately after descending the hump. Maximum speeds less than 10 mph are sought, but exceedances of 10 mph are likely, and protective devices such as tank car head shields and shelf couplers have been designed to withstand the effects of humping speeds up to 18 mph (Orringer and Tong, 1980). The tank shell and sills are

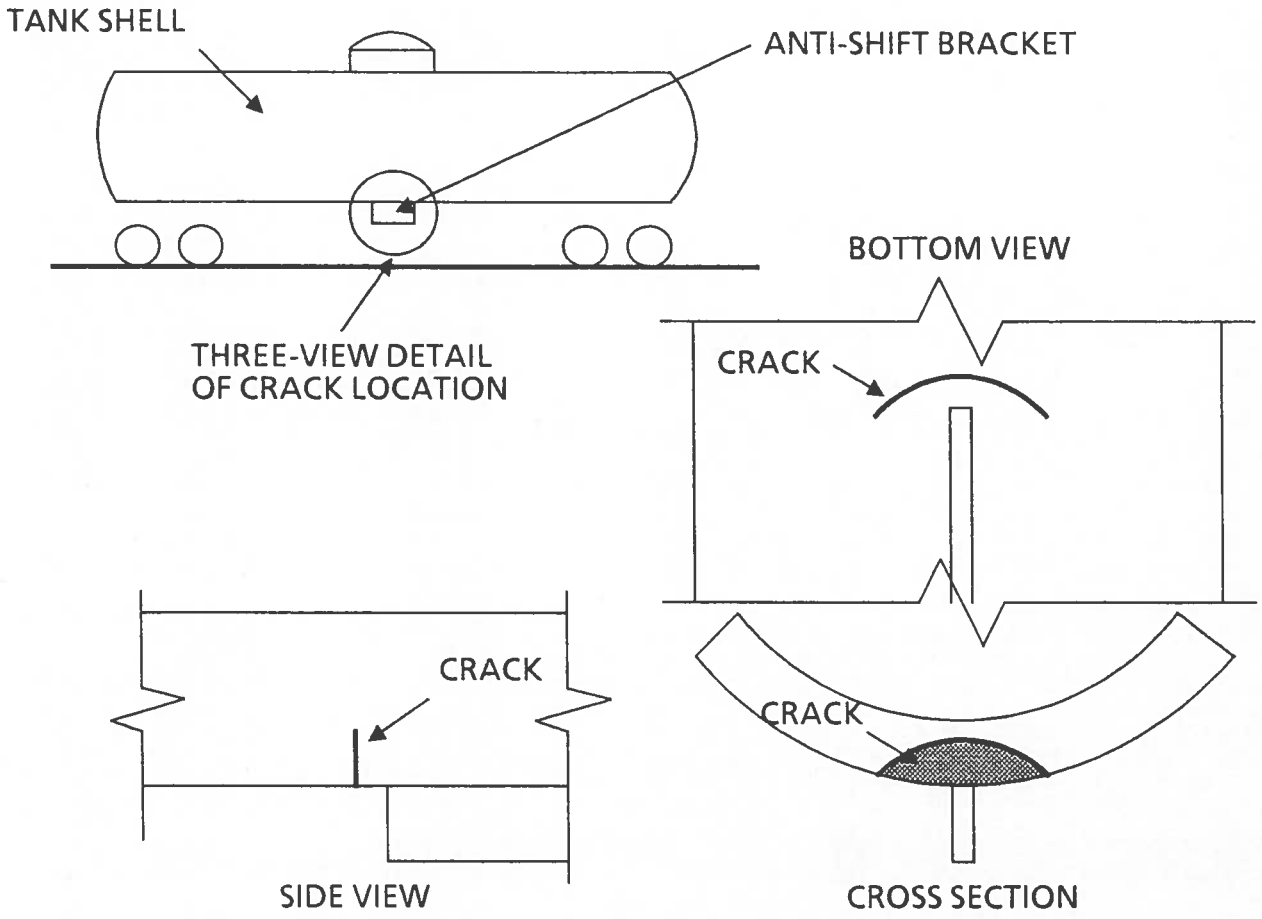

FIGURE 1. RAIX 7033 CRACK LOCATION AND ORIENTATION

designed to specifications requiring that the car structure withstand an impact compression load of 1.25 million pounds and a static tension load of 350,000 pounds (Anon., 1982). The compression load is intended to simulate the peak dynamic load corresponding to a worst-case humping incident, and the tension load is intended to represent the worst case of coupler runout to full draft during train operations.

Following the RAIX 7033 shell crack discovery, the Federal Railroad Administration (FRA) Office of Safety began an investigation of the circumstances associated with the crack. Examination of the hardware revealed that the anti-shift brackets had not been welded to the car shell in conformance with the specification in effect for hazardous material tank cars when the car was manufactured.

The purpose of the anti-shift bracket is to hold an outer jacket and insulation layer in place. The brackets thus transfer reaction loads from the insulation and jacket into the shell when the car is subjected to accelerations caused by coupling or by runout during train operations. The local shell stresses from such loads are concentrated by the corner detail at the shell-to-bracket connection. Residual stresses are also present as a result of the welding process. The design detail specification requires insertion of a pad between the shell and bracket when the length of weld around the bracket exceeds 6 linear inches. The purpose of this specification is to relieve the shell by increasing the area available for load transfer (Figure 2A). The anti-shift bracket on RAIX 7033 was not in conformance with the specification because the pad had been omitted (Figure 2B), although the length of weld around the bracket was 25 inches.

The FRA Office of Safety further established that the shop drawings for the group of cars that included RAIX 7033 specified the non-conforming detail shown in Figure 2B. Other groups of hazardous material tank cars were then reviewed by the industry, and some of these groups were also found to have shop drawings that specified the non-

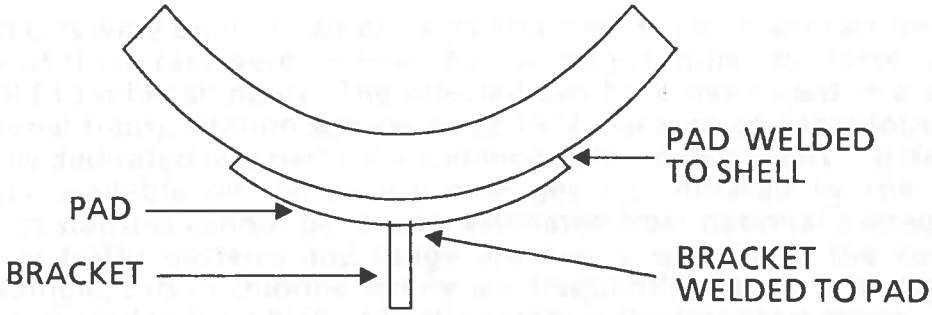

(A) SPECIFICATION FOR DETAIL

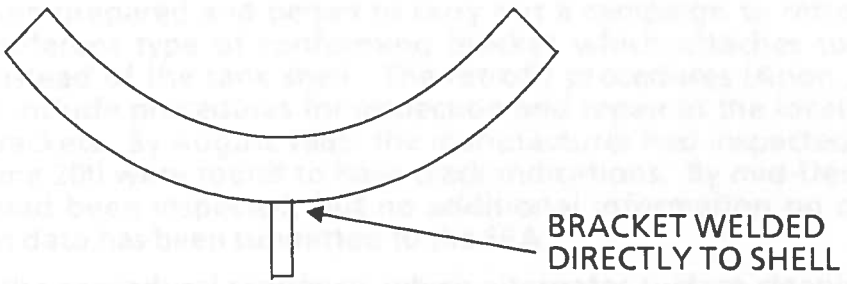

(B) NON-CONFORMING DETAIL

FIGURE 2. ANTI-SHIFT BRACKET DETAILS

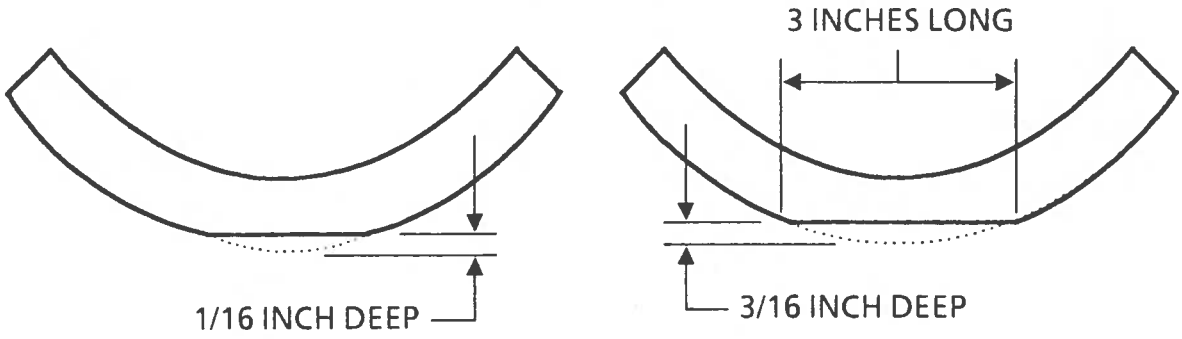

(A) LIMIT FOR REPAIR BY GRINDING ONLY

(B) LIMIT FOR WELD REPAIR WITHOUT X-RAY OR STRESS RELIEF (NON-PRESSURE CARS)

FIGURE 4. GRINDING LENGTH AND DEPTH LIMITS

by X-ray and stress-relieved after weld repair. Also, cars that have been weld repaired are subjected to a hydrotest.

The manufacturer's procedures specify that weld repairs are to be made by arc-gouging the damaged area to remove the crack, back-filling with weld metal, and grinding to restore the surface contour. The repair is required to be performed from both inside and outside the shell to assure complete weld penetration (see Figure 5). The procedure follows established industry practice (Anon., 1982).

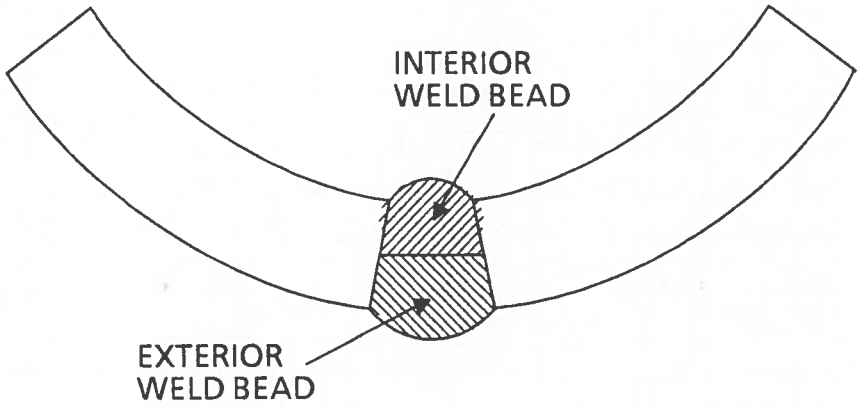

FIGURE 5. WELD REPAIR REQUIREMENTS

The manufacturer's procedures incorporate Appendix R of the AAR Manual of Standards and Recommended Practices (Anon., 1982) by reference but do not specify the heat treatment for stress relief. Appendix R permits local heat treatment for non-pressure cars but requires unit heat treatment for pressure cars. Unit heat treatment means that the entire structure must be placed in an oven to achieve uniform temperature during the stress relief process. Appendix R refers to Appendix W for specifications relating to qualification of both welders and welding procedures. The detail and quality of the standards set forth in Appendix W conform to the provisions of an accepted national standard for welding (Anon., 1977).

The manufacturer's immediate action to inspect, repair, and return the affected cars to service reflects two strong incentives. First, the current average cost of a new tank car is estimated to be $75,000. Hence, the 9,000 affected cars represent a capital investment of nearly $700 million in terms of replacement cost if these cars were to be permanently removed from service. Second, the total U.S. freight fleet includes about 70,000 tank cars possessing the classifications and capacities (20,000 to 33,000 gallons) for safe and efficient transportation of the hazardous chemicals required by the nation's industries. The 9,000 affected cars thus represent over 10 percent of the nation's transportation capacity, and even temporary removal from service has the potential to create a serious bottleneck in the nation's production. These are compelling reasons to return the cars to service as quickly as possible, provided that doing so does not entail unacceptable risk to the health and safety of railroad employees and the public.

On August 29, 1985, in the light of the concern about safety, the FRA Associate Administrator for Safety requested that the DOT Transportation Systems Center (TSC) make a preliminary assessment of the adequacy of the manufacturer's inspection and repair procedures and report the results of the assessment. On August 30, TSC organized an assessment task force consisting of five senior faculty members from three universities, a National Bureau of Standards expert on the mechanical properties of tank car steels, two senior members of the Center's technical staff, and additional supporting staff. The eight members of the task force are nationally recognized authorities in the fields of metallurgy, mechanical engineering, structures, structural fatigue, and fracture mechanics.

The task force met at TSC on September 13 to review the pertinent information from FRA files and the open literature and to establish criteria for the assessment. The task force met again at TSC on October 18 to review the results of calculations made by the supporting staff and to formulate conclusions.

The following section discusses the assessment criteria and results. Section 3 presents the task force conclusions and recommendations. Appendices A through C contain the details of the supporting calculations. The sources used by the task force are collected in the bibliography (Appendix D). The composition of the task force and supporting staff appears in Appendix E.

2. Assessment

Three elements of risk must be considered if a hazardous material tank car fleet that has experienced shell cracking is to be returned to hazardous material service. These risks involve fatigue crack growth in the normal service environment, bursting failures under conditions that a nominal car would survive, and the potential for weld repairs to increase the fleet exposure to the first two risks.

The first risk is that undetected cracks in cars returned to service might later cause failures. If the inspection procedure does not detect 100 percent of the cracks present in the fleet at any given time, the undetected cracks might continue to grow in fatigue during subsequent service. A circumferential crack, such as was found in RAIX 7033, is susceptible to service fatigue from axial dynamic bending stresses. Periodic inspection is required to reduce this risk. Section 2.1 deals with this issue.

The second risk is that local reductions of shell thickness might lead to burst failures. A burst failure is possible when a tank car is engulfed in a fire. The scenario for such events begins with a derailment and puncture of a tank car containing a flammable liquid. A fire almost invariably follows the puncture and engulfs adjacent tank cars. A large-scale conflagration results if the adjacent tank cars burst. Section 2.2 discusses the relation between effective shell thickness and risk of burst.

The third risk is that a weld repair might damage the shell if the repair procedure is not adequate. The damage might escape detection and become a growing fatigue crack. A small initial crack might eventually be detected by periodic inspection, but one must consider the risk of an initial crack large enough to progress to failure before the next inspection. Section 2.3 discusses this questions.

2.1 Crack detection

Two of the four inspection-repair pathways shown in Figure 3 depend entirely on the dye penetrant method for crack detection. Of the roughly 3,000 cars that were inspected by August 1985, about 2,800 cars with no crack indications have followed one of these pathways, and some of the remaining 200 might have followed the second. Similar figures can be expected for the rest of the campaign. Thus, the integrity of the affected fleet depends mainly on the effectiveness of the dye penetrant inspection.

To limit the inspection to one time per car, as in the current procedure, is to assume that the dye penetrant method finds every crack. Consideration of the dye penetrant method and its application to the affected cars makes this assumption questionable.

Figure 6 illustrates the dye penetrant inspection concept. The surface to be inspected is first swabbed with a flourescent dye; if a surface crack is present, a small amount of the dye enters the crack by capillary action. The surface is then cleaned, leaving the dye in the crack. The dry surface is then covered with a hygroscopic powder which reabsorbs some of the dye from the crack. When the surface is illuminated with ultraviolet light, the reabsorbed dye flouresces and outlines the crack.

The ability of the dye penetrant method to detect cracks depends on the properties, state of stress, and surface condition of the material being inspected. Material properties can influence the capillary action to some extent, compressive stress can close the crack mouth, and some surface conditions can interfere with the capillary action. For any specific application, these factors place a lower limit on the size of a crack that can be detected with a given reliability. This limit ("detectable crack size" or "detectability limit") is usually defined in terms of the crack mouth length along the surface. Some but not all cracks shorter than the detectable size can be found, but the detection reliability decreases as the crack length decreases (see Figure 7).

To find the detectability limit for a given application requires a blind experiment on samples containing cracks whose sizes are independently determined either by non-

destructive inspection with better resolution than the dye check or by sectioning and direct physical measurement on the crack surface. Such an experiment on aircraft alloys gave 100 percent detectable sizes for the dye penetrant method of 0.25 inch for aluminum and 0.35 inch for a high strength steel (Packman et al., 1969). This experiment was performed on small samples in a laboratory environment, however, conditions more favorable for crack detection than can be expected in a shop environment. With regard to the affected tank cars, the effectiveness of the first dye check might be reduced by surface grit not completely removed by wire brushing, and

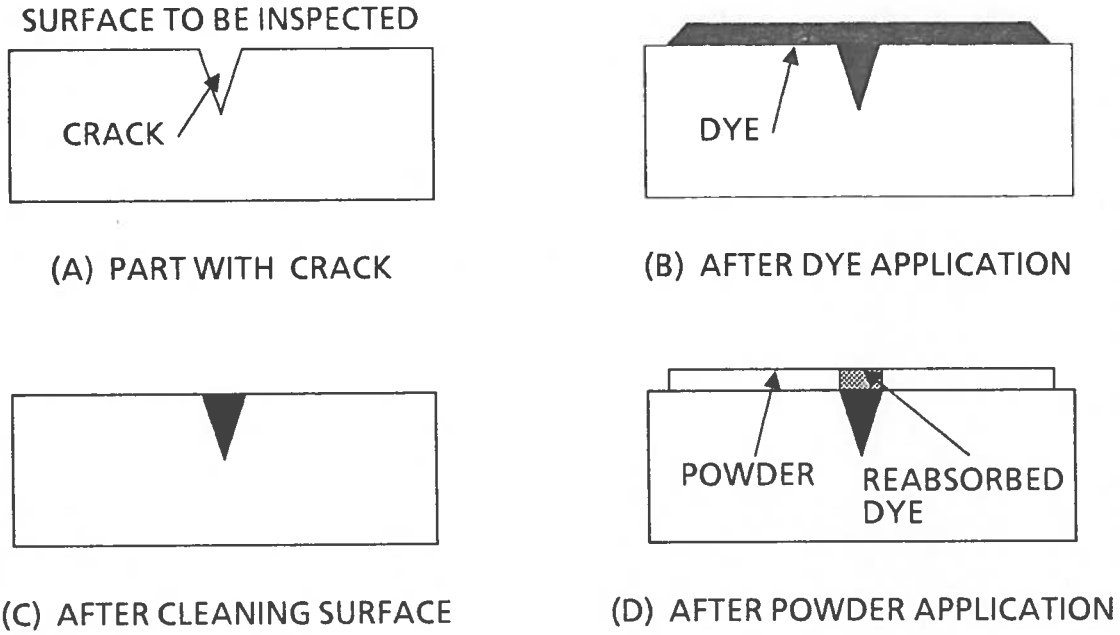

FIGURE 6. THE DYE PENETRANT METHOD

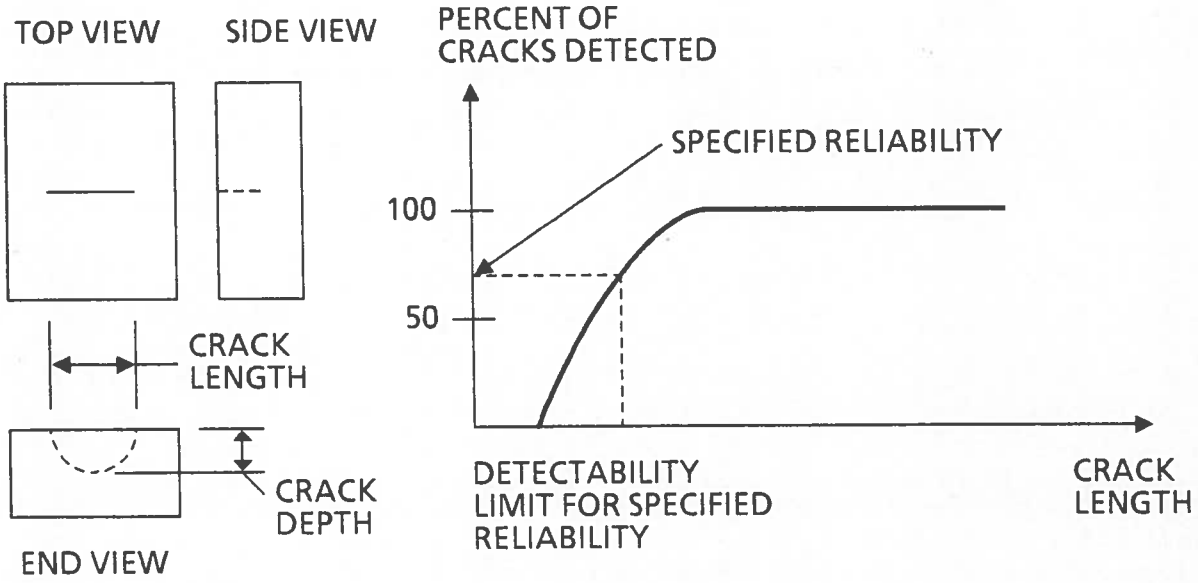

FIGURE 7. DETECTION RELIABILITY VERSUS CRACK LENGTH

the effectiveness of the second dye check might be reduced because of metal smeared over the crack mouth by the grinding process (see Figure 3). Conversely, existing standards for dye penetrant inspection usually assume a separate clean station at the end of a parts production line (Marsh et al., 1976; Anon., 1983).

It is also important to recognize that the detectable size is only an estimate. The empirical definition of the detectability limit is the shortest crack length for which every crack in the experiment is found. If there were 24 such cracks in the test, for example, and the test were extended or the method applied, chances are that the 25th and succeeding cracks would also be found. This outcome cannot be assumed, however, and the most one can conclude with certainty from the detection of 24 test cracks is that the reliability is at best 24/25 (96 percent) at the empirical detectability limit.

In the light of the foregoing factors, the task force saw no justification for assuming that the manufacturer's dye check procedures would find every crack, and that a detectability limit of 0.5 inch would be conservative but reasonable for the given circumstances. This assumption is consistent with a survey of dye penetrant inspection results in aircraft maintenance facilities, for example, which showed that 50 percent of the 0.5-inch cracks could be detected with 95 percent confidence (Lewis, 1978), and a 50 percent detectable 0.5-inch crack was used in the present analysis. To assure the continued integrity of the affected cars in service then requires periodic inspection at intervals governed by the rate at which an undetected crack will grow in fatigue. Fatigue life is determined by the number of service stress cycles required to grow a crack from the detectability limit to the size at which the next stress cycle can be expected to cause either cracking through the shell wall or unstable fracture. For the present case, the detectability limit is defined to be a semi-elliptical surface crack with the dimensions shown in Figure 8. This definition corresponds to an undetected quench crack that has been rapidly deepened by a local residual stress field resulting from the original bracket weld.

Fatigue crack growth life was calculated from established material crack growth properties for low-carbon steels (Rolfe and Barsom, 1977), fracture toughnesses estimated from Charpy test data for tank car steels (Interrante, 1976; Pellini, 1983), handbook stress intensity factor formulae for surface cracks (Campbell et al., 1975), and established methods for service fatigue stress description and crack growth calculation (Orringer,1984a,b). The service loads for tank cars were obtained from the results of operational tests for dynamic loads (Johnson, 1978) and fire safety simulations for tank car internal pressure versus temperature (Johnson, 1984).

Safe inspection intervals were defined to allow 13 opportunities to detect the crack during its calculated fatigue life. This meets the objective used for definition of safe airframe inspection intervals to protect the flight crews and passengers in military airplanes (Military Specification, 1972) and commercial transport category airplanes

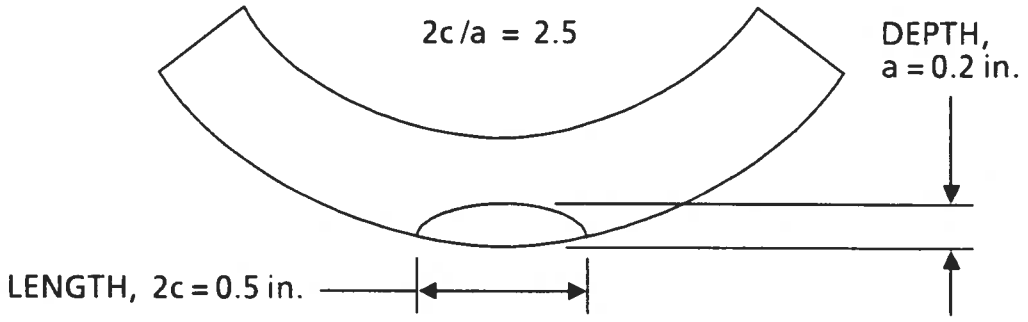

FIGURE 8. DETECTABILITY LIMIT USED FOR ANALYSIS

(Anon., 1978; 14 CFR 25.571, 1984). The level of risk implied by adoption of the safe inspection intervals calculated for the affected tank cars is thus equivalent to the risk currently accepted for aircrews and airline passengers.

Appendix A contains the details of the analysis. The safe interval depends primarily on the tank shell wall thickness. However, cars with 7/16-inch walls carrying ethylene oxide constitute a special case because this commodity is normally pressurized during transport. Also, the critical crack size for 9/16 wall cars was found to be smaller than the detectable size (see Appendix B), and this commodity has been excluded from the inspection interval calculations for cars with 9/16-inch walls. Table 2 summarizes the results by wall thickness and car type.

TABLE 2. CALCULATED SAFE INSPECTION INTERVALS

Wall Thickness (in.)	7/16	7/16	9/16	11/16
Car type	111A/100W CARRYING ETHYLENE OXIDE	111A/100W CARRYING OTHER PRODUCTS	105A/100W 105A/200W 112A/200W EXCEPT PROPYLENE	105A/300W 105A/400W 105A/500W 112A/340W 112A/400W 112A/500W
Safe Interval (miles)	5,000	15,000	205,000	1,015,000

2.2 Bursting strength

Tank car shells are required to meet minimum standards for nominal wall thickness and burst pressure (49 CFR 179.101-1 and 201-1, 1984). In cases governed by the burst pressure requirement, the required thickness, t, is determined by assuming a uniaxial state of hoop stress (49 CFR 179.100-6, 1984):

$$t = \frac{Pd}{2SE} \tag{1}$$

where P is the burst pressure requirement, d is the inside diameter, S is the minimum ultimate tensile strength of the tank material (49 CFR 179.100-7, 1984), and E is a weld efficiency factor.‡ Equation 1 is conservative in that it does not take advantage of the favorable effect of the biaxial stress state induced by internal pressure. Therefore, the actual burst pressure for a nominal shell designed in accordance with Equation 1 will be somewhat higher than the required burst pressure. Table 1, in Section 1, summarizes the burst pressure requirement by car type for the cars in the affected population.

Each tank must be hydrostatically tested after construction (49 CFR 179.100-18 and 200-22, 1984) to a test pressure corresponding to the "slash number"(e.g., a DOT-112A/340W car must be tested to 340 psig) The tank is equipped with a relief valve set below the test pressure. The burst pressure requirement is thus intended to provide a margin of safety for overheating, e.g., if a tank car is engulfed in a fire. Fire engulfment can occur when an adjacent tank car carrying a flammable commodity is punctured in a derailment. Under normal conditions, the engulfed car will vent its contents in a controlled manner. Test experience has shown, however, that the

‡For tank heads with seams, $E = 0.9$; otherwise $E = 1.0$ is allowed.

internal pressure may exceed the normal vent pressure and the shell strength may be degraded by high temperatures on dry wall areas if the car is overturned (Johnson, 1984). Hence, it is necessary to consider pressure and temperature conditions corresponding to fire engulfed overturned cars when making an assessment of the risk of bursting. The present analysis uses the conditions corresponding to dry wall after 100 minutes of fire engulfment, as calculated in simulations (Johnson, 1984). The 100-minute point was chosen because it constitutes the survivable limit specified for DOT-112 and -114 cars (49 CFR 179.105-4, 1984) and is the only specific standard of this type to which reference can be made.

If the shell thickness is locally reduced, either by grinding or by the presence of a crack, the burst pressure and safety margin will be correspondingly reduced. The task force was asked to evaluate this reduction as a function of effective thickness.

To address the question of grinding, the task force assumed that the grinding process would remove any crack present in the shell. Burst pressure was then calculated for the biaxial stress state due to internal pressure by equating the corresponding Mises-Hencky equivalent stress to the material ultimate strength at the applicable dry wall temperature (see Appendix B). No factor of stress concentration was assumed, since prior yielding of the material would eliminate such concentrations. The worst case is for A212/A515 materials, for which the ultimate strength is 70,000 psi. TC128 normalized material, with 81,000 psi ultimate strength, would give better performance.

Table 3 summarizes the results by comparing the manufacturer's specified grinding limit with the calculated depths at which the survivable limit would just be achieved. In each case the survivable limit is at least four times the specified limit, i.e., a car would have to be overground by more than 3/16 inch and returned to service with no other action before it would fail to meet the CFR pool fire survivability standard. Failure to detect and correct this amount of overgrinding is considered to be extremely unlikely.

TABLE 3. COMPARISON OF GRINDING LIMITS

TYPE OF LIMIT	7/16-INCH WALL	9/16-INCH WALL	11/16-INCH WALL
Manufacturer's normal allowance (1/16)	0.062	0.062	0.062
Pool fire survivability limit	0.290	0.250	0.270

Long-term corrosion might also contribute to the reduction of wall thickness. The literature on corrosion engineering tends to concentrate on general environments to which a wide variety of structures are subjected, e.g., moisture, moist air, seawater, and seawater with low concentrations of various common chemicals. The accepted engineering practice for average steels in such environments is to assume a corrosion rate of 0.001 inch depth of surface attack per year (Uhlig, 1971). Applying this assumption to the affected tank cars leads to an order-of-magnitude estimate of 0.02 inch loss of wall thickness to date (0.001 inch/year × 2 surfaces × 10 years of service). If applied as a penalty factor, the estimated loss to date would not change the foregoing conclusions on safe inspection interval or burst resistance. If a total useful tank car life of 30 to 40 years is considered, the corresponding estimate of 0.06 to 0.08 inch of wall thickness loss begins to be of concern. The task force concern in this area is

whether the actual corrosion rates and wall losses will be greater than the estimate and, if so, by how much.

The commodities that may cause interior attack are concentrated chemicals, some of which may be highly corrosive to tank car steels. On the other hand, the shell exterior may be exposed to condensates that are trapped between the shell and the insulation as the cars are alternately exposed to hot humid and cold dry environments. Such condensates would form primarily from water vapor, but should be expected to contain dilute sulfites, sulfates, carbonates, and other acid or hydrocarbon radicals that the water vapor has entrained from polluted urban air environments.

The effective shell thickness can also be reduced by the presence of an undetected crack. Under the conditions of fire temperatures, the shell material would be highly ductile, and a crack would fail by plastic instability. Both the elastic fracture mechanics method (Appendix A) and the net section method (Appendix B) were used to estimate the crack depth for which the instability would occur at overturned car pressure. These estimates serve to define the critical crack sizes that determine the end of calculated fatigue life. A plastic fracture mechanics model has been developed to treat this type of problem more accurately than the simple theories and has been applied to cracks in line pipe steels (Erdogan, 1982). The material properties data required for application of this model to tank car steels is not available, but the estimates bracket the accurate result and give almost identical calculated fatigue lives.

2.3 Weld repair

For detected cracks that cannot be removed by grinding within the stated limit, the manufacturer's procedures require repairs in accordance with the provisions of Appendix R of the industry standards for tank cars (Anon., 1982). Appendix R requires that such repairs be made by arc-gouging‡ the cracked region to remove the crack and back-filling with weld metal both outside and inside the shell (see Figure 5), followed by post-weld heat treatment for stress relief. The work is required to be performed by qualified welders who are subject to annual recertification by independent welding inspectors.

The task force notes that a strict reading of Appendix R would require unit post-weld heat treatment for repairs to pressure cars. Unit heat treatment means that the entire tank shell is subjected to elevated temperature in a large oven. While the unit heat treatment procedure is undoubtedly followed when weld repairs are made to bare tank shells on the production line, the task force questions whether the unit procedure can be applied to the present service repairs without damaging the insulation. The requirement for unit heat treatment may be unnecessary for these service repairs if it can be shown from past experience that such repairs have been routinely made with local heat treament and that the repaired cars have continued in service without any abnormal incidence of weld failures.

Appendix R also refers to Appendix W for specifications covering the qualification of welders and welding procedures. The specifications in Appendix W conform to the ASME Pressure Vessel and Boiler Code (Anon., 1977) , a nationally accepted standard for welding practices. The welding procedure must be qualified by means of standard tests for the mechanical properties and documented by means of a written welding procedure specification (WPS). These practices assure consistency and quality but cannot guarantee that every weld made in accordance with the WPS will be free of defects. Repair welds are of special concern in this respect because the manual procedures used to make such welds do not allow precise control to the parameters of the WPS.

‡Appendix R also permits other removal methods, but the builder's procedures require arc-gouging.

In view of the foregoing factors, the task force cannot rule out the possibility that one or more cars that have been repaired by welding might contain a defect that could develop into a fatigue crack after the car is returned to service. Small defects would grow relatively slowly in fatigue and can be controlled by the periodic reinspection program discussed in Section 2.1. The isolated occurrence of a large defect is also possible, and such a defect might cause a service failure before the first reinspection. The manufacturer's inspection and repair procedures protect against this possibility in most cases by means of stress relief and X-ray check. However, the additional protection is not required for weld-repaired non-pressure cars, provided that they have not been ground more than 3/16 inch deep or 3 inches long (see Figure 3 in Section 1).

3. Conclusions and Recommendations

3.1 A single nondestructive inspection cannot be counted on to find every crack in a fleet; for cracks that are found and are repaired, the possibility of collateral damage during the repair weld cannot be ruled out. A prudent response requires that the affected fleet be assumed to contain cracks when it is returned to service, and that periodic reinspection be performed to provide additional opportunity to detect and safely remove or repair cracks before they can propagate to failure under service fatigue stresses. The body of this report has focused, therefore, on the estimation of safe inspection intervals.

3.2 The initial inspection found cracks in only a small percentage of the affected fleet. Therefore, it is reasonable to consider the question of how extensive the periodic reinspections should be. The answer depends on the risk involved in a tank car shell failure that might result from propagation of an undetected crack. The task force finds two distinct levels of risk, depending on the commodity carried.

3.3 Highly toxic and/or flammable commodities entail the risks of major explosion and/or major public health hazard. Commodities in this category include all liquefied flammable gases, anhydrous ammonia, ethylene oxide, and other liquids that readily vaporize to create inhalation hazards. The task force concludes that the possibility of even a single failure of a car carrying one of these commodities should not be tolerated. The task force consequently recommends that 100 percent of the cars carrying these commodities be reinspected at each interval.

3.4 Other hazardous commodities, such as acids, do not pose the risks of explosion or immediate inhalation hazard but do pose a risk of local environmental damage in the spill area. The task force concludes that the risk of a single failure is tolerable for this category, but that the risk of repeated failures should not be tolerated. Therefore, the task force recommends that a small number of cars carrying these commodities be sampled at each interval, and that a 100 percent inspection be performed if a crack is found in the sample. The objective of the limited-sample inspection is to provide early warning in the event that the fleet still contains a number of cracks comparable to the number found during the initial inspection. A sample of 150 cars per interval will establish 95 percent confidence that the program will identify the specified situation (see Appendix C).

3.5 Both reinspection programs require removal of insulation, cleanup, and dye check of the shell at the former bracket locations. The safe inspection interval depends on the shell thickness and ranges from 5,000 service miles for DOT-111A/100W cars carrying ethylene oxide to one million service miles for the pressure cars with 11/16-inch wall thickness. The task force recommends that these inspection intervals be applied to the affected fleet.

3.6 Propylene requires special consideration. Propylene is a liquefied flammable gas that can be carried in cars with 9/16 and 11/16 walls, according to current regulations. For the 9/16-inch wall, calculations based on the simulation of an overturned fire engulfed car carrying propylene showed that a loss of more than 0.15 inch of the wall section would render the car unable to meet the existing standard for survival of 100 minutes of a pool fire (see Appendix B). Although this standard officially covers only DOT-112 and -114 cars, the task force considers it appropriate to apply because of the special circumstances of the present case and the risk category of propylene. Considered as a critical crack size, the 0.15-inch section loss is less than the 0.2-inch detectable crack size, i.e., a safe inspection interval based on fatigue crack growth cannot be defined for this case. Also, the 0.15-inch section loss is only slightly more than twice the allowable 1/16-inch grinding depth for cars that can be returned to service without other repair actions. Thus, it is possible that small measurement errors might place a 9/16 wall back in service with a section overground close to the pool fire

survivability limit. Therefore, the task force recommends that affected cars with 9/16-inch walls be restricted from carrying propylene.

3.7 The task force is not able to evaluate the quality of weld repairs. The quality is believed to be sufficient to preclude any risk of high incidence of collateral damage being introduced into the affected fleet as a result of the repair procedures; however, the task force recommends that the FRA confirm this belief by reviewing existing reports of similar repairs and cross-indexing these reports with accident records. A documented record of numerous repairs with little or no incidence of weld fatigue failures would confirm the quality. Should the weld quality not be confirmed, the task force additionally recommends that the stress relief and X-ray check procedures (applied to all pressure cars and some non-pressure cars that were weld-repaired) should be extended to all weld-repaired non-pressure cars that carry highly toxic and/or flammable commodities as one method of precluding the early fatigue failure of any isolated large defect that might otherwise pose a major safety risk.

3.8 Long-term corrosion over the remaining useful life of the affected cars might cause sufficient additional reduction of wall thickness to place an overground shell at risk of burst in the overturned car scenario, if the rate of shell corrosion is large in comparison with generic corrosion rates on other structures. The task force recommends that the tank car industry engage in research to determine the specific rates of corrosion on tank car shells subjected to both hazardous commodities and the railroad ambient environment.

Appendix A - Service Stress and Crack Growth Estimates

Fatigue crack growth in metals is characterized by specimen tests. In each test, a specimen containing a sharp crack is subjected to a number of identical stress cycles sufficient to establish the rate of crack growth in terms of the stress ratio, R, and stress intensity factor range, ΔK:

$$R = \frac{S_{min}}{S_{max}} \qquad \Delta K = [G(a)\sqrt{a}]\,\Delta S \tag{A-1}$$

where S_{min} and S_{max} are respectively the minimum and maximum stress in the cycle,

$$\Delta S = S_{max} - S_{min} \tag{A-2}$$

is the stress range, a is the measure of crack size, and $G(a)$ is a function of the crack shape and boundary geometry. For a fixed stress ratio, the crack growth rate data generally plot as shown in Figure A-1, and the mid-ΔK fatigue regime can be modelled by the crack growth rate equation:

$$\frac{da}{dN} = \frac{C(\Delta K)^m}{1-R} \tag{A-3}$$

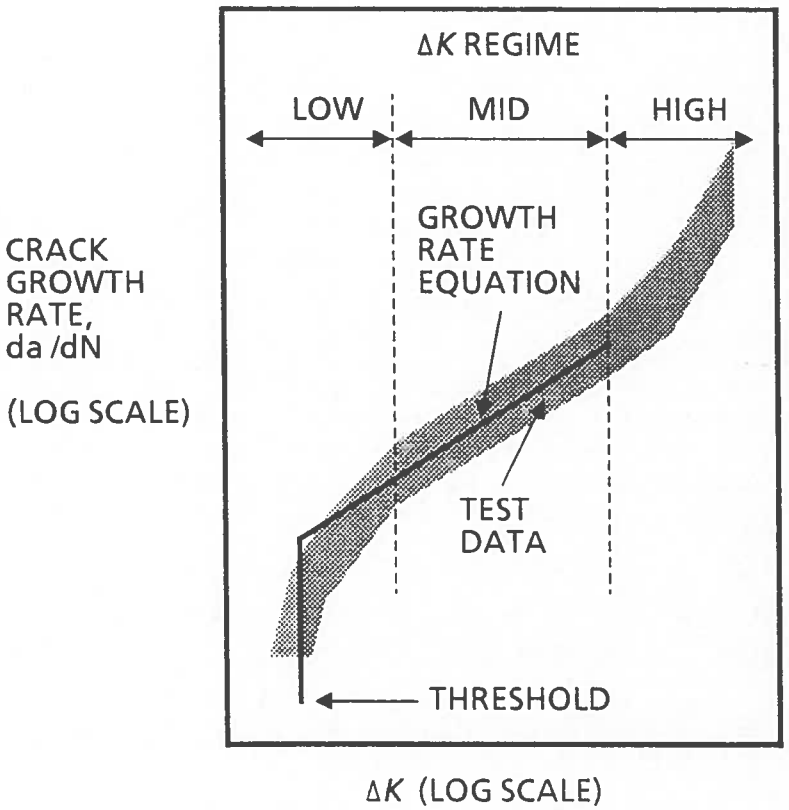

FIGURE A-1. TYPICAL FATIGUE CRACK GROWTH RATE BEHAVIOR

where the parameters C and m are determined from the experimental data. Equation A-3 is considered to describe the material behavior whenever ΔK exceeds a threshold value given by:

$$\Delta K_{TH} = (1 - R)\,\Delta K_{TH0} \tag{A-4}$$

where ΔK_{TH0} is the experimentally determined threshold for $R = 0$. Rate equations different from Equation A-3 are sometimes used to model the high- regime, but this regime is of no interest in the present analysis.

Behavior in the mid-ΔK regime is generally insensitive to material strength and toughness properties. Therefore, published data for low-carbon steels can be used to estimate crack growth rates for tank car steels, which have chemical compositions and microstructures similar to the steels that have been tested. A widely accepted mid-ΔK crack growth rate equation for such steels (Rolfe and Barsom, 1977) is given by:

$$\frac{da}{dN} = \frac{3.6 \times 10^{-10} (\Delta K)^3}{1 - R} \qquad \Delta K_{TH0} = 7 \tag{A-5}$$

where da/dN is in units of inch/cycle and ΔK is in units of ksi$\sqrt{}$inch. Equation A-5 is used in the present analysis.

The handbook crack geometry function for a semi-elliptical surface flaw in a flat plate (Campbell et al., 1975) is used in the present application. This function is given implicitly by:

$$G(a) = 1.12 M_K \sqrt{\frac{\pi}{Q}} \tag{A-6}$$

where Q and M_K are functions of the crack depth a. The flaw shape parameter Q depends on the ratio of crack dimensions $a/2c$ and the ratio of maximum stress S_{max} to material yield strength S_Y; the deep flaw magnification factor M_K depends on Q and the ratio of crack depth to specimen thickness.

Figure A-2 graphically describes these functions. The interval $0.2 \leqq S_{max}/S_Y \leqq 0.56$ covers the stress cycles expected for a circumferential crack in a tank car shell (see later discussion). For the assumed shape $a/2c = 0.4$, the average values $Q = 2.0$ and $M_K = 1.05$ reasonably represent the flaw. The M_K value is an average over approximately 80 percent of the crack growth life (see later discussion).

Strictly speaking, the geometry factors embodied in Equation A-6 and Figure A-2 apply only to the elastic regime, i.e., when the zone of plastic deformation at the crack front is small compared with the specimen thickness. In practice, however, the plastic zone will be large when S_{max}/S_Y is large or when the crack depth approaches the specimen thickness (Figure A-3). The geometry factors should also include a correction for the curvature of the shell. Both the plastic zone and the curvature effect have been accounted for in a study of circumferential surface cracks in gas transmission pipelines (Erdogan, 1982). The results of this study show that the curvature correction is not significant for shells whose diameter and wall thickness correspond to tank car dimensions. The plastic zone effect is significant for deep cracks but the corresponding correction can be neglected, as explained later, without introducing any serious error into the fatigue life calculation.

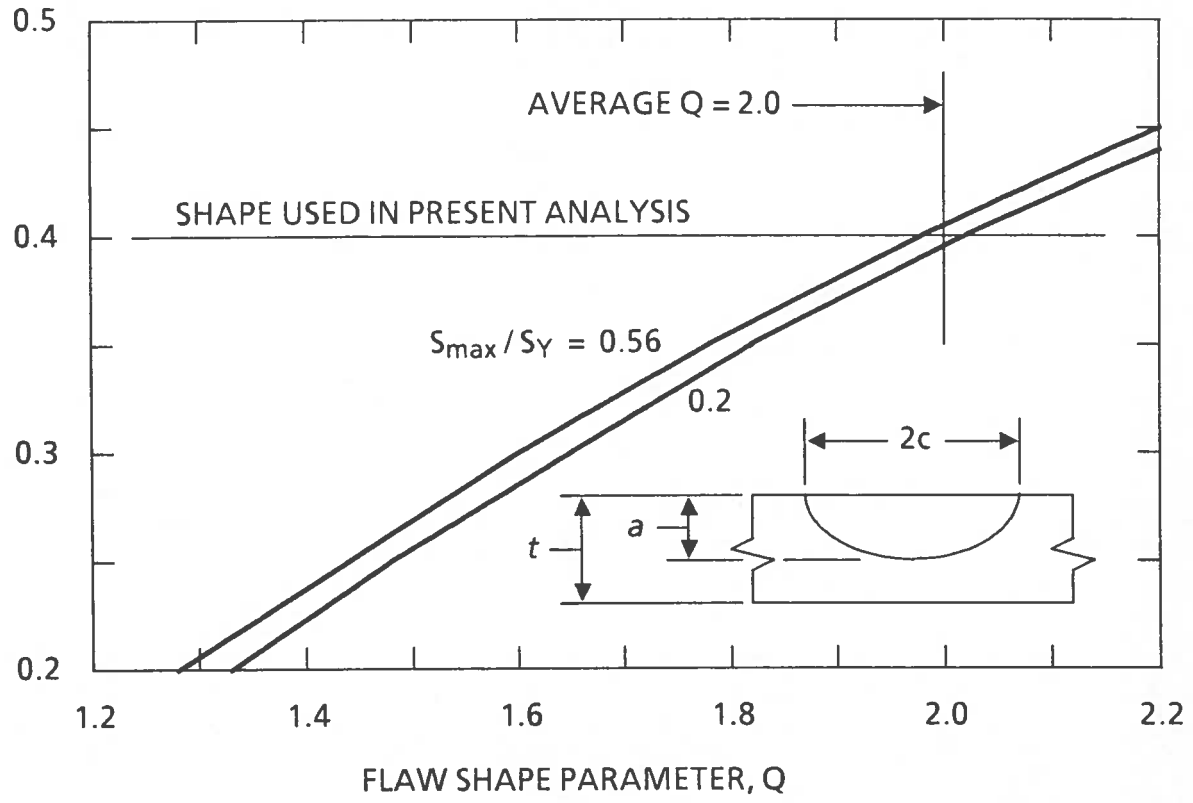

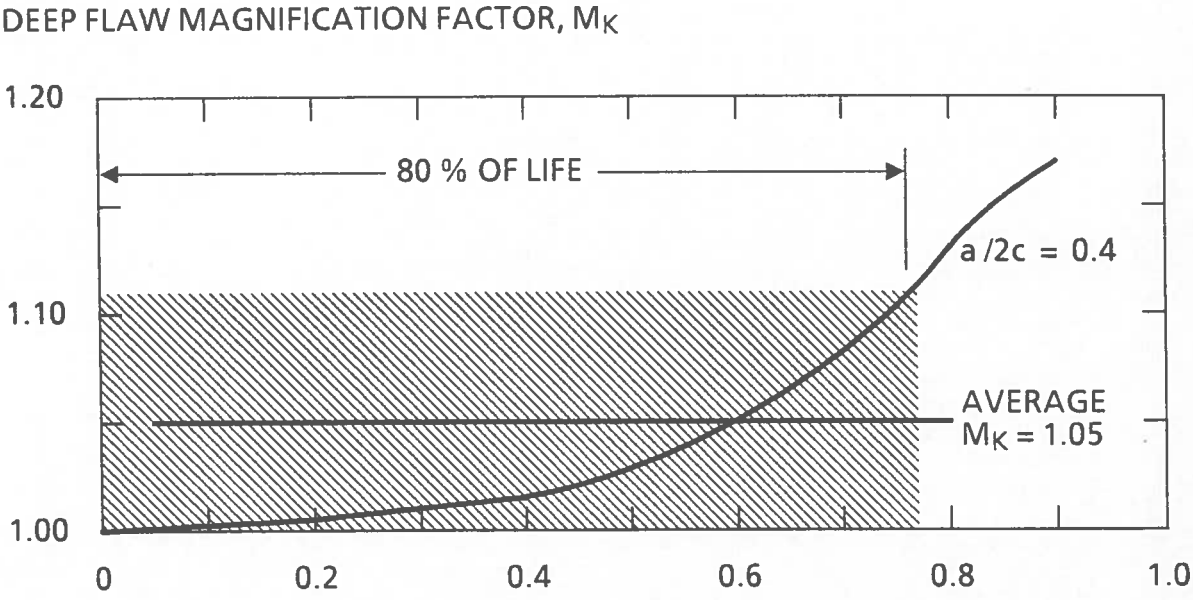

FIGURE A-2. SURFACE FLAW GEOMETRY FUNCTIONS
(Abstracted from Campbell et al., 1975)

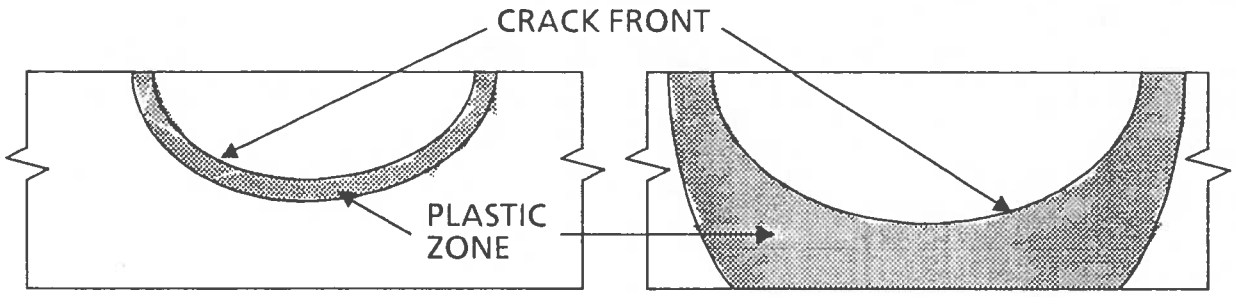

(A) ELASTIC FRACTURE MECHANICS APPLIES

(B) ELASTIC FRACTURE MECHANICS DOES NOT APPLY

FIGURE A-3. PLASTIC ZONE SIZE

To calculate a service fatigue life requires that the crack growth increment per cycle, as given by the rate equation, be summed for all stress cycles in the service loading history. With the service stress cycles organized into repeating blocks, the sum extends over the number of blocks required to grow the crack from a defined initial size a_0 to a defined critical size a_{cr}. The number of such blocks is then the calculated fatigue life.

The initial crack size in the present case is the detectability limit for periodic inspection (see Figure 8 in Section 2.1). The critical crack size is qualitatively defined as that size for which a structural failure can be expected when the next service load is encountered. The quantitative definition of critical crack size generally requires investigation of two or more conditions of service loading (see later discussion).

When the stress intensity factor formula is combined with the crack growth rate equation (Eqs. A-1, A-3 and A-6), the crack increment sum can be formally solved for the calculated fatigue life L in terms of two integrals (Orringer, 1984a,b):

$$L = \frac{\int_{a_o}^{a_{cr}} \frac{da}{[G(a)\sqrt{a}]^m}}{C\int \frac{(\Delta S)^m n(\Delta S, R)\, d(\Delta S)}{1-R}} \qquad \text{(A-7)}$$

where $n(\Delta S, R)d(\Delta S)$ represents the stress cycle occurrence rate. For example, $nd(\Delta S)$ might be expressed in terms of the expected number of occurences per mile of the stress ranges between ΔS and $\Delta S + d(\Delta S)$, with the corresponding stress ratio implied. The fatigue life calculated from Equation A-7 would then be in miles. In practice, both integrals in the life equation can be computed by trapezoid sum approximations. This approach has been used to estimate the safe crack growth lives of structural details in an urban bus undercarriage (Orringer and Tong, 1985).

For the present case, the approximations of constant Q and M_K lead to the following simple expression for the crack geometry integral:

$$\int_{a_0}^{a_{cr}} \frac{da}{[G(a)\sqrt{a}]^m} = \frac{1}{[1.12 \times 1.05\sqrt{\pi/2}]^3} \int_{a_0}^{a_{cr}} a^{-3/2}\, da = 0.625 \left[\frac{1}{\sqrt{a_0}} - \frac{1}{\sqrt{a_{cr}}} \right] \quad \text{(A-8)}$$

The value $M_K = 1.05$ is found by applying Equation A-8. Since the calculated fatigue life is proportional to the crack geometry integral, and since a_{cr} cannot exceed the wall thickness in any case, the crack depth at 80 percent of life can be estimated as:

$$a_{80\%} = \frac{1}{[0.8(\frac{1}{\sqrt{a_0}} - \frac{1}{\sqrt{t}}) - \frac{1}{\sqrt{a_0}}]^2} \quad \text{(A-9)}$$

The ratio a/t then varies between 0.82 and 0.73 as the wall thickness increases from 7/16 to 11/16 inch, and the average M_K value represents this regime (Figure A-2).

The tank car service environment is described in terms of mechanical loads and tank pressures that must be converted into stress descriptions. The normal service environment encompasses static load, dynamic bending loads encountered during train operations, hump yard loads, and internal pressures up to normal vent pressure. Also, internal pressures and temperatures corresponding to overtuned cars engulfed in pool fires must be considered as part of the process of estimating critical crack size. Each environment component is described below; the critical crack size estimates then follow.

Static load is based on a fully loaded 33,000-gallon capacity tank car. The pressure-to-stress conversion is based on a 112-inch tank diameter; the axial component of the pressure stress is:

$$S_P = \frac{PD}{4t} \quad \text{(A-10)}$$

where P is the internal pressure and D is the tank diameter, and the hoop-stress component is $2S_P$. The weight of the car and lading is converted to static bending stress based on the dimensions for the 25,000-gallon capacity car shown in Figure A-4. The sill height and spans are representative of cars in the 25,000 to 33,000-gallon range. In the present analysis, the generic car is treated as a total load $W = 240$ kips uniformly distributed over a span $\ell = 53$ feet. Stub-sill construction is assumed, and the tank shell stress at midspan is then calculated from the formula for a uniformly loaded simply supported beam:

$$S_{ST} = \frac{W\ell^2}{2\pi D^2 t} \quad \text{(A-11)}$$

The midspan stress is considered to be a conservative but reasonable estimate for the stress at a former bracket location.

The dynamic loads are obtained from operational tests (Johnson, 1978) in which a 33,000-gallon DOT-112A tank car truck bolster was strain-gaged and calibrated for truck load (static load $W/2 = 120$ kips). The dynamic environment was measured as exceedings per mile of load levels above and below the static load; Figure A-5 reproduces the data and depicts the procedure used to estimate range-mean pairs

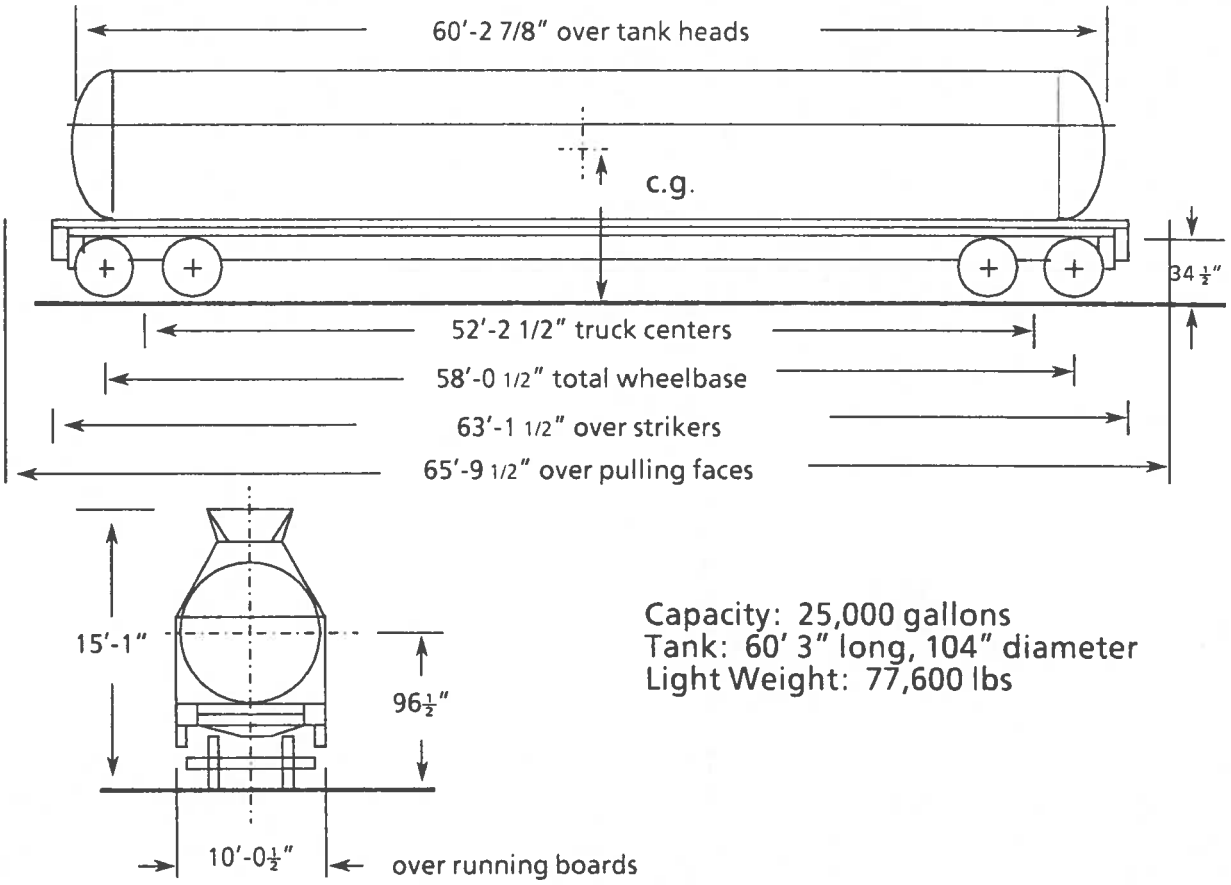

FIGURE A-4. TANK CAR GN 100095 , TYPE 111A/100W1 (From Combes, 1970)

from the level exceedance curves. The interpretation of this diagram is that load ranges ΔL_{AV} (with corresponding mean L_{AV}) occur at the frequency per mile given by:

$$dn(\Delta L_{AV}, L_{AV}) = (e_1 - e_2)(\Delta L_2 - \Delta L_1) \tag{A-12}$$

This interpretation reflects an assumption that the dynamic loads constitute a narrow band process and a conservative assumption that the two truck loads acting on a tank shell are in phase. Table A-1 summarizes the load range-mean pair occurrences obtained from Figure A-5.

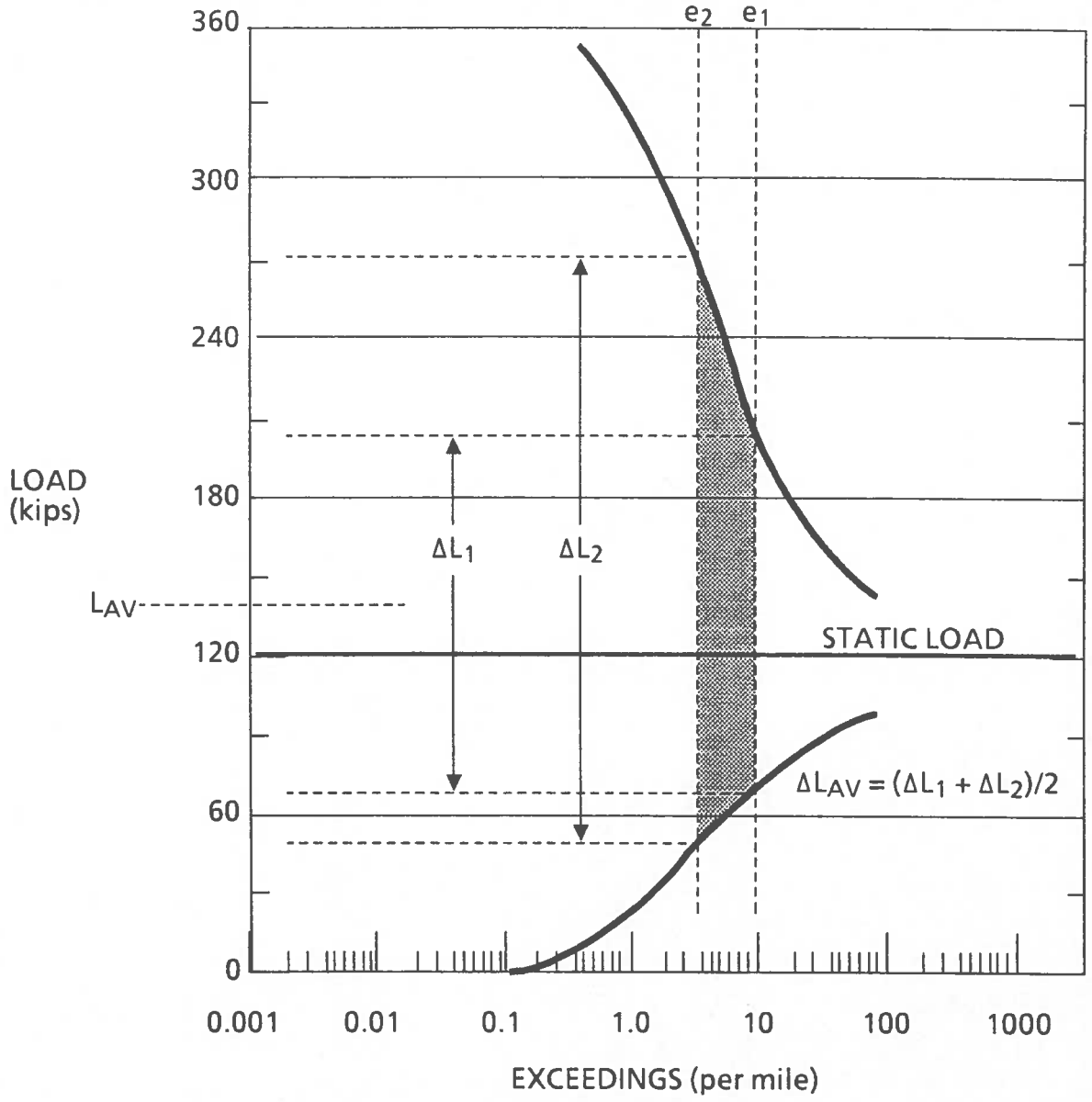

FIGURE A-5. TANK CAR TRUCK LOAD EXCEEDANCES

TABLE A-1. LOAD EXCEEDANCE AND OCCURRENCE SUMMARY

EXCEED-ANCE RANGE (per mile)	TRUCK LOADS (kips)				OCCUR-RENCES (per mile)	TRUCK LOADS (kips)	
	ABOVE MEAN		BELOW MEAN				
	LOW	HIGH	HIGH	LOW		RANGE	MEAN
80-70	140	142	95	93	10	45-49	117.50
70-60	142	144	93	91	10	49-53	117.50
60-50	144	151	91	89	10	53-62	118.75
50-40	151	156	89	87	10	62-69	120.75
40-30	156	162	87	85	10	69-77	122.75
30-20	162	165	85	78	10	77-87	122.50
20-10	165	184	78	68	10	87-116	123.75
10-9	184	188	68	65	1	116-123	126.25
9-8	188	195	65	62	1	123-133	127.50
8-7	195	200	62	60	1	133-140	129.25
7-6	200	208	60	58	1	140-150	131.50
6-5	208	215	58	56	1	150-159	134.25
5-4	215	232	56	48	1	159-184	137.75
4-3	232	274	48	44	1	184-230	149.50
3-2	274	315	44	38	1	230-277	167.75
2-1	315	318	38	29	1	277-289	175.00
1-0.9	318	320	29	27	0.1	289-293	173.50
0.9-0.8	320	330	27	25	0.1	293-305	175.50
0.8-0.7	330	334	25	23	0.1	305-311	178.00
0.7-0.6	334	338	23	22	0.1	311-316	179.25
0.6-0.5	338	343	22	19	0.1	316-324	180.50
0.5-0.4	343	350	19	17	0.1	324-333	182.25
0.4-0.3	350	355	17	12	0.1	333-343	183.50
0.3-0.2	355	360	12	6	0.1	343-354	183.25

The static load was converted to shell bending stress by means of beam theory (see Equation A-11). Stress range-mean pairs corresponding to the dynamic loads are obtained by assuming that the shell bends dynamically in a single symmetric mode. Under this assumption, the stress data can be calculated from the proportional relations,

$$\frac{\Delta S_{AV}}{S_{ST}} = \frac{\Delta L_{AV}}{W/2} \qquad \frac{S_{AV}}{S_{ST}} = \frac{L_{AV}}{W/2} \tag{A-13}$$

and the stress ratio is then given by:

$$R = \frac{S_{AV} - \frac{1}{2}\Delta S_{AV}}{S_{AV} + \frac{1}{2}\Delta S_{AV}} \qquad \text{(A-14)}$$

Table A-2 summarizes the occurrence data ΔS, S_{AV}, and dn (ΔS, S_{AV}) for each wall thickness. The pressure stress S_P must be added to S_{AV} and R must be recalculated, however, before carrying out the stress spectrum integral in Equation A-7.

TABLE A-2. DYNAMIC STRESS SPECTRA FOR SHELLS

OCCURRENCES (per mile)	7/16-INCH WALL		9/16-INCH WALL		11/16-INCH WALL	
	ΔS_{AV} (ksi)	S_{AV} (ksi)	ΔS_{AV} (ksi)	S_{AV} (ksi)	ΔS_{AV} (ksi)	S_{AV} (ksi)
10	1.705	4.265	1.322	3.3045	1.0767	2.6918
10	1.85	4.265	1.4345	3.3045	1.1684	2.6918
10	2.09	4.315	1.617	3.3397	1.3173	2.7204
10	2.38	4.385	1.842	3.3959	1.5005	2.7762
10	2.65	4.45	2.053	3.4522	1.7233	2.81205
10	2.98	4.45	2.306	3.4451	1.8785	2.8063
10	3.685	4.495	2.8545	3.4803	2.3253	2.8349
1	4.34	4.585	3.36075	3.5506	2.7376	2.8922
1	4.65	4.63	3.5998	3.5858	2.9323	2.9209
1	4.955	4.695	3.83885	3.63495	3.1271	2.9609
1	5.265	4.775	4.0779	3.6983	3.3218	3.0125
1	5.61	4.875	4.34505	3.7755	3.5394	3.0755
1	6.23	5.00	4.8232	3.874	3.9288	3.1557
1	7.52	5.43	5.8215	4.2045	4.7421	3.4248
1	9.205	6.09	7.1295	4.7177	5.8074	3.8429
1	10.275	6.355	7.959	4.9216	6.4832	4.009
0.1	10.57	6.30	8.184	4.8794	6.6664	3.975
0.1	10.86	6.375	8.409	4.9357	6.8497	4.0204
0.1	11.185	6.465	8.662	5.006	7.0559	4.0777
0.1	11.385	6.51	8.8165	5.041	7.1819	4.1064
0.1	11.62	6.555	8.995	5.0765	7.3308	4.135
0.1	11.93	6.62	9.2385	5.1255	7.5225	4.1751
0.1	12.275	6.66	9.5055	5.1605	7.7431	4.2038
0.1	12.655	6.655	9.801	5.1535	7.9837	4.198

Hump yard loads are isolated, i.e. they occur at the rate of one or two loads per thousand service miles. No statistics are available on hump yard load magnitudes because the magnitudes are sensitive to the car's mass and impact speed at the instant of coupling with a standing consist (Orringer and Tong, 1980). The performance

requirements to which tank car shells are designed include the ability to withstand an impact compression load of 1.25×10^6 pounds and a static tension load of 350,000 pounds (Anon., 1977). The design compression load implicitly defines the worst hump load that is considered non-abusive and is, therefore, an appropriate bounding value in the absence of operational data. The design load is applied along the coupler centerline (Figure A-6).

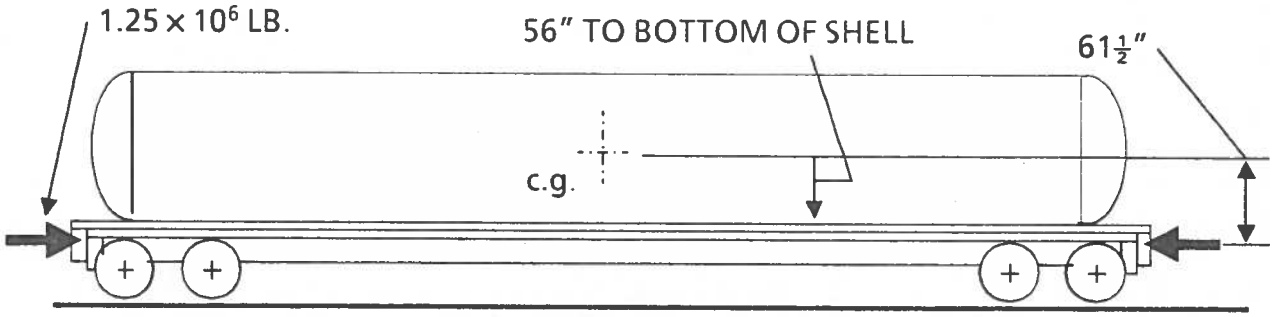

FIGURE A-6. DESIGN HUMP LOAD

In the present analysis, the net compression plus beam bending stress at the bottom of the shell is calculated by treating the design load as a static load. Although this stress is compressive, it is assumed to characterize the magnitude of a dynamic stress wave which is reflected through the shell as tension. Such a tension wave might have caused the final breaching of the RAIX 7033 shell. Table A-3 summarizes the total (static plus dynamic) stresses estimated by this calculation.

TABLE A-3. DESIGN MAXIMUM STRESSES DUE TO SEVERE HUMPING

Component	7/16-Inch Wall	9/16-Inch Wall	11/16-Inch Wall
Static Bending	6.665	5.16	4.20
Dynamic Compression	8.088	6.284	5.136
Dynamic Bending	6.632	5.146	4.20
Total (ksi)	21.385	16.59	13.536

Internal pressure creates axial tension S_P and hoop tension $2S_P$ in the tank shell, where:

$$S_P = \frac{PD}{4t} \qquad \text{(A-15)}$$

in terms of the pressure P, shell diameter D, and wall thickness t. The internal pressure varies with the temperature of the tank car and the commodity carried and is limited by the normal vent pressure unless the car has been overturned. Test and accident experience with overturned cars has shown that even a normally operating relief valve

is not able to vent liquid at a rate sufficient to keep the internal pressure at its normal limit, and that *P* may exceed the normal vent pressure. The overpressures that govern each case have been obtained from simulations of tank cars engulfed in fires (Johnson, 1984), as explained in Appendix B. Normal service pressure is generally well below normal vent pressure. Normal service pressures can be estimated from the results of the simulations. Table A-4 summarizes the key pressures and corresponding shell stresses. The service stress and pressure in this table were selected to represent average ambient conditions in which the tank and its contents are 30 Fahrenheit degrees warmer than the zero-pressure point. This corresponds to an ambient temperature of about 90°F.

TABLE A-4. PRESSURE AND PRESSURE-STRESS SUMMARY

Item	7/16-Inch Wall	9/16-Inch Wall	11/16-Inch Wall
Governing Commidities	1,3-Butadiene† Ethylene oxide‡§	Vinyl Chloride† Propane‡	Propylene†‡
Service Pressure (psig)	5, 75§	10	30
Vent Pressure (psig)	75	150	300
Overpressure (psig)	150	400	550
Service Stress, S_P (ksi)	0.3225, 4.84§	0.5027	1.2368
Vent Stress, S_P (ksi)	4.84	7.54	12.37
Overstress, S_P (ksi)	9.60	19.91	22.40

†Determines service pressure ‡Determines critical crack size §See text

Ethylene oxide carried in cars with 7/16-inch walls presents a special case. This commodity is normally pressurized with nitrogen gas when transported, and the gas pressure is close to the design vent pressure. Therefore, the safe fatigue crack growth life for ethylene oxide cars will be less than the life for non-pressure cars carrying other commodities.

The safe life for fatigue crack growth is considered to end when the size of the crack is such that it will propagate unstably through the shell wall in the next stress cycle. The instabilty point is determined either by a fracture criterion based on the maximum survivable hump load or by plastic rupture based on pool fire conditions. Both criteria involve strength properties of the shell material. The shells of the affected cars were constructed with either A515 Grade 70 or TC128 normalized steel alloy, the properties of which are summarized in Table A-5.

The ultimate tensile strength of a material governs the strength of structures that fail by plastic collapse, e.g., as in the bursting of a nominal tank car shell. The property is specified by regulation (49 CFR 179.100-7, 1984). The Charpy V-notch test is an indirect measure of a material's resistance to fracture when stress is applied to a sharp crack. The data quoted in Table A-5 were obtained from existing studies of tank car steels (Interrante, 1976; Pellini, 1983). Charpy test results for low-carbon steels in the strength range represented by A515 and TC128 can be used to estimate the dynamic fracture toughness K_{Id} according to the following empirical formula developed by means of parallel Charpy and fracture toughness tests (Rolfe and Barsom, 1977):

TABLE A-5. MATERIAL STRENGTH PROPERTIES

Property	A515 Grade 70	TC128 normalized
Yield strength, S_Y (ksi)	38	50
Ultimate tensile strength, S_U (ksi)	70	81
CVN† energy, lower shelf (ft.lb.)	3	3
CVN† energy, upper shelf (ft.lb.)	30.8	55.4
Lower-shelf toughness, K_{Id} (ksi√in.)‡	21.2	21.2
Upper-shelf toughness, K_{Id} (ksi√in.)‡	68	91
Transition temperature (°F)	+ 30	– 30

†Charpy V-notch test. ‡Estimated from CVN data (see text).

$$K_{Id}^2 = 5E(CVE) \tag{A-16}$$

where E is Young's modulus (3×10^7 psi for steel), CVE is the Charpy test energy in ft.lb., and the result for K_{Id} is in psi√inch. Critical crack sizes for elastic fracture are determined by solving:

$$K_{max} = S_{max} G(a_{cr}) \sqrt{a_{cr}} = K_{Id} \tag{A-17}$$

for the crack size when a maximum service stress S_{max} is inserted in the stress intensity factor formula. The upper and lower shelf terminology reflects the fact that fracture toughness depends on the material's temperature, as shown in Figure A-7. Table A-5 also lists the transition temperatures.

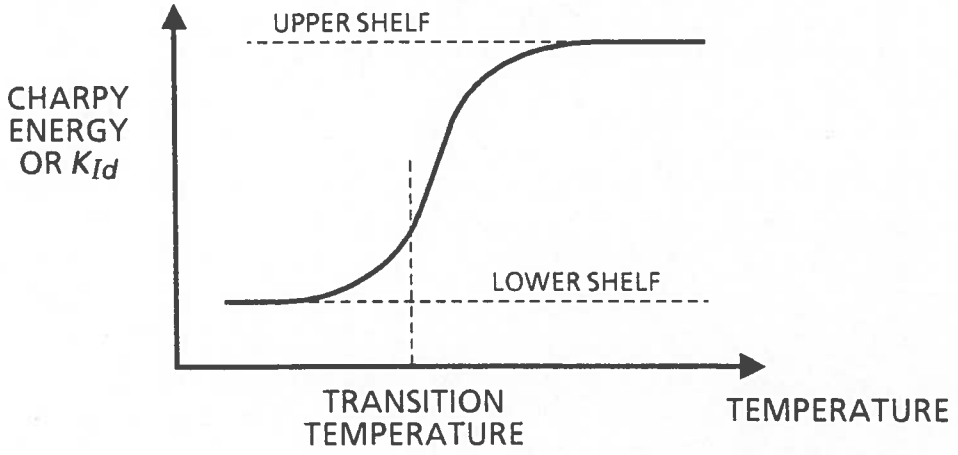

FIGURE A-7. TOUGHNESS VERSUS TEMPERATURE TRANSITION

The task force understands that the majority of the affected tank cars were constructed with A515 Grade 70 steel. Therefore the analysis is based on A515 Grade 70 properties where these are inferior to the corresponding properties of TC128 steel.

For the purpose of fatigue crack growth calculation, a circumferential crack in the shell of the generic tank car was assumed to be subjected to static and dynamic service bending stress plus the axial stress due to service pressure, as defined in Table A-4. The resultant range-mean pairs were allowed to contribute to the stress spectrum integral only if the corresponding ΔK exceeded ΔK_{TH} at the critical crack size.

The possible fatigue crack growth of axial cracks was also considered by assuming that the crack would be subjected to diurnal stress cycles $(\Delta S, R) = (2S_P, 0)$ corresponding to service pressure. However, these cycles were well below the threshold for crack growth, and the analysis was consequently limited to circumferential cracks.

Critical crack size was determined as the smallest of the crack sizes calculated by the following methods:

- Elastic fracture ($K_{max} = K_{Id}$) for lower-shelf toughness and for the design maximum humping stress given in Table A-3.
- Net section rupture (see Appendix B) for the stresses due to overpressure.

Both methods make the pessimistic (i.e., conservative) assumption that a worst-case event occurs as soon as the crack has grown to the minimum depth at which the event can cause a failure. The first calculation qualitatively represents situations like the RAIX 7033 incident at North Little Rock. The second calculation represents an overturned car that would burst due to overpressure, as contrasted with a nominal car that would survive the overpressure. Table A-6 summarizes the results of these calculations and includes the results for the crack geometry integral (Equation A-8).

Both estimates for critical crack size could have been made based on the plastic fracture mechanics model mentioned earlier (Erdogan, 1982), were the appropriate material properties data available. However, this model requires measurements of fracture toughness in terms of crack opening displacement, an approach that has been adopted to date only for extremely ductile materials such as pipeline steels. Such calculations would likely give critical crack sizes slightly larger than the elastic fracture estimates and slightly smaller than the net section rupture estimates. In any case, a small error in the critical crack size has almost no effect on the calculated fatigue life because the crack grows at a rapid rate as it approaches the critical size.

TABLE A-6. CRITICAL CRACK DEPTHS AND CRACK GEOMETRY INTEGRAL

Method	7/16-Inch Wall	9/16-Inch Wall	11/16-Inch Wall
Elastic fracture, a_{cr} (in.)	0.43	0.56	0.68
Net section rupture, a_{cr} (in.)	0.29	0.25	0.27
Crack geometry integral	0.237	0.148	0.195

Table A-7 summarizes the service stress spectra (static and dynamic bending plus service pressure stress) and the results for the stress spectrum integral (denominator of Equation A-7). Stress range-mean pairs for which $\Delta K < \Delta K_{TH}$ were not included in the stress spectrum integral and have been omitted from Table A-7.

TABLE A-7. SERVICE STRESS SPECTRA

OCCURRENCES (per mile)	7/16-INCH WALL Ethylene oxide		7/16-INCH WALL Other		9/16-INCH WALL		11/16-INCH WALL	
	ΔS (ksi)	*R*	ΔS (ksi)	*R*	ΔS (ksi)	*R*	ΔS (ksi)	*R*
10	1.705	0.829						
10	1.850	0.816						
10	2.090	0.795						
10	2.380	0.771						
10	2.650	0.750						
10	2.980	0.724						
10	3.685	0.670						
1	4.340	0.626						
1	4.650	0.606						
1	4.955	0.588						
1	5.265	0.570						
1	5.610	0.552						
1	6.230	0.519						
1	7.520	0.464	7.520	0.209				
1	9.205	0.407	9.205	0.184				
1	10.275	0.371	10.275	0.130				
0.1	10.570	0.356	10.570	0.112				
0.1	10.860	0.348	10.860	0.105	8.409	0.128		
0.1	11.185	0.338	11.185	0.096	8.662	0.120		
0.1	11.382	0.332	11.382	0.091	8.8165	0.114		
0.1	11.620	0.325	11.620	0.084	8.995	0.107		
0.1	11.930	0.317	11.930	0.076	9.2385	0.098	7.5225	0.180
0.1	12.275	0.304	12.275	0.064	9.5055	0.087	7.7431	0.168
0.1	12.655	0.290	12.655	0.049	9.801	0.071	7.9837	0.153
INTEGRAL	8368.6		3490.8		150.01		38.61	

The foregoing results assume a service fatigue life uninterrupted by severe humps. A second calculation was made to assess the effects of repeated severe hump loads, using the tensile stress corresponding to the 1.25×10^6-lb. design load. Table A-8 summarizes the calculated fatigue lives for service loads alone, hump loads alone, and combined loads assuming one hump load per thousand service miles. Safe inspection intervals corresponding to the last case are shown at the bottom of the table. These inspection intervals are derived by taking one 1/13 of the calculated fatigue life and rounding the result to the nearest five thousand miles. This procedure generally follows the practice applied to protect aircrews against fatalities resulting from airframe fracture in military airplanes (Military Specification, 1972) and is in line with similar regulations imposed by the Federal Aviation Administration for the protection of aircrews and passengers in transport category commercial airplanes (14 CFR 25.571,

1984). The task force opinion is that an equivalent practice is called for in the present case in order to reduce the risk of a hazardous material accident in the affected fleet to a level that has been accepted in other transportation sectors that involve the risk of fatalities. The general objective of these practices is to establish inspection intervals that assure a high confidence of detecting a crack within its safe fatigue crack growth period. In the present case, the task force judged that a 0.9999 confidence would be sufficient. This confidence level means a one in 10,000 chance of missing a crack, i.e., expectation of a miss for less than one of the 9,000 affected cars. Since the probability for detecting a 1/2-inch surface crack in one inspection is 0.5 (see Section 2.1), the number of inspections r per safe period is given by the probability equation:

$$1-(1-0.5)^{r}=0.9999 \qquad \text{(A-18)}$$

After rounding to the nearest whole number, $r = 13$ is obtained from the solution of Eq. A-18.

TABLE A-8. FATIGUE LIFE AND SAFE INSPECTION INTERVAL SUMMARY

Item	7/16-Inch Wall Ethylene oxide	7/16-Inch Wall Other	9/16-Inch Wall Except Propylene	11/16-Inch Wall
Service fatigue life (miles)	78,667	188,591	2,740,558	14,029,181
Hump load life (number)	67,316	67,316	90,037	218,404
Combined life (miles)	78,575	188,064	2,659,605	13,182,409
Safe inspection interval (mi.)	5,000	15,000	205,000	1,015,000

Appendix B - Strength Estimates for Reduced Thickness Shells

The geometric discontinuities associated with a ground area of a shell wall concentrate the wall stresses when the stresses are elastic. If the stresses exceed the material yield strength, local plastic strain first occurs at the stress concentration points, and the material's ductility begins to even out the stress distribution. If the section becomes fully plastic, the stress concentration decreases further and disappears as the material approaches its ultimate strength (see Figure B-1). Hence, bursting strength should be based on a uniform stress equal to the material's ultimate strength.

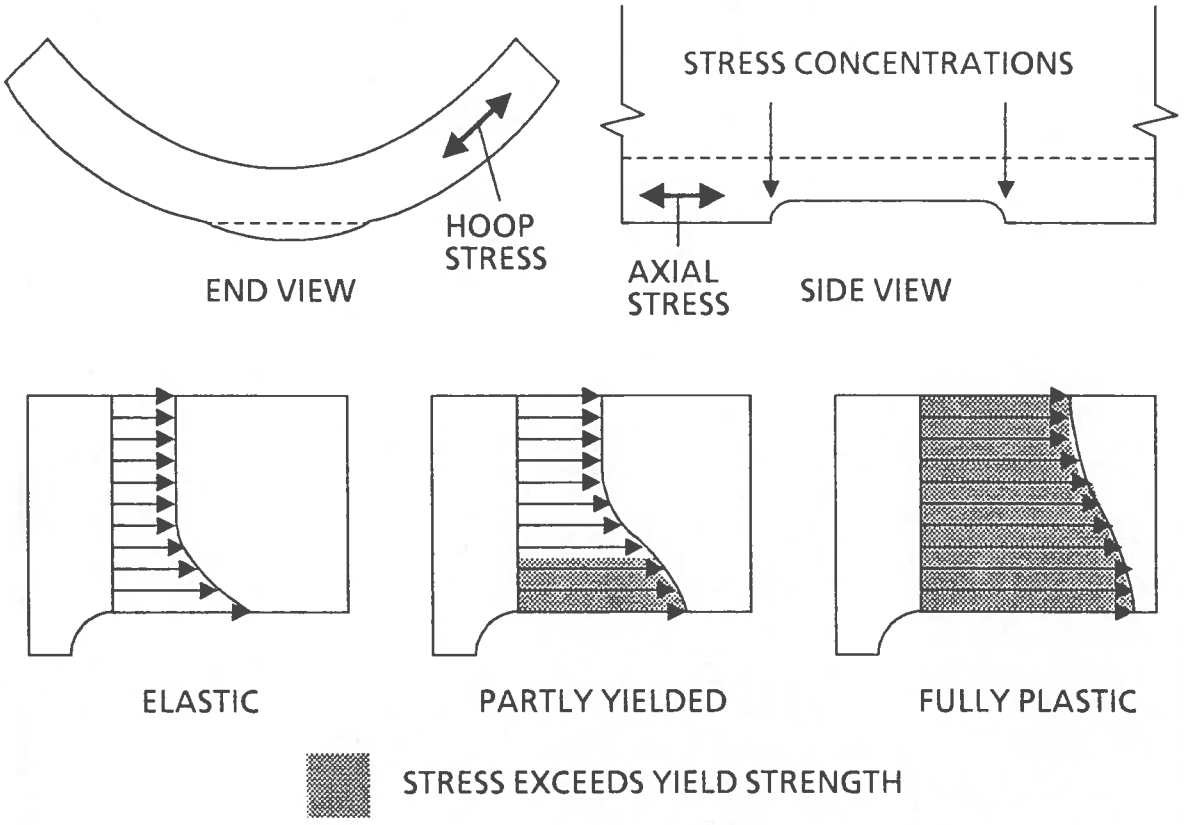

FIGURE B-1. EFFECT OF PLASTICITY ON STRESS CONCENTRATION

In the present case, bursting of a tank car shell is controlled by pressure stresses which are much greater than the mechanical stresses when an overturned car is subjected to a fire and vent overpressure. The internal pressure causes both axial stress $S_1 = S_P$ and hoop stress $S_2 = 2S_P$, where:

$$S_P = \frac{PD}{4t} \tag{B-1}$$

in terms of the pressure P, shell diameter D, and wall thickness t. The biaxial stress state delays the onset of yielding. For example, most ductile metals tend to follow the Mises-Hencky yield criterion (McClintock and Argon, 1966); for biaxial stress states, this criterion is given by:

$$S_1^2 + S_2^2 + (S_1 - S_2)^2 = 2S_Y^2 \tag{B-2}$$

where S_Y is the material yield strength. Equation B-2 describes the elliptical yield locus shown in Figure B-2. When a material is stressed beyond its yield strength and unloaded, experiments show that the yield locus is expanded, i.e., Equation B-2 can be applied to a subsequent loading event by replacing S_Y with the increased yield strength that resulted from the work hardening. Hence, it is reasonable to apply Equation B-2 to the calculation of bursting strength, with the material ultimate strength S_U replacing S_Y, i.e.:

$$S_1^2 + S_2^2 + (S_1 - S_2)^2 = 2S_U^2 \tag{B-3}$$

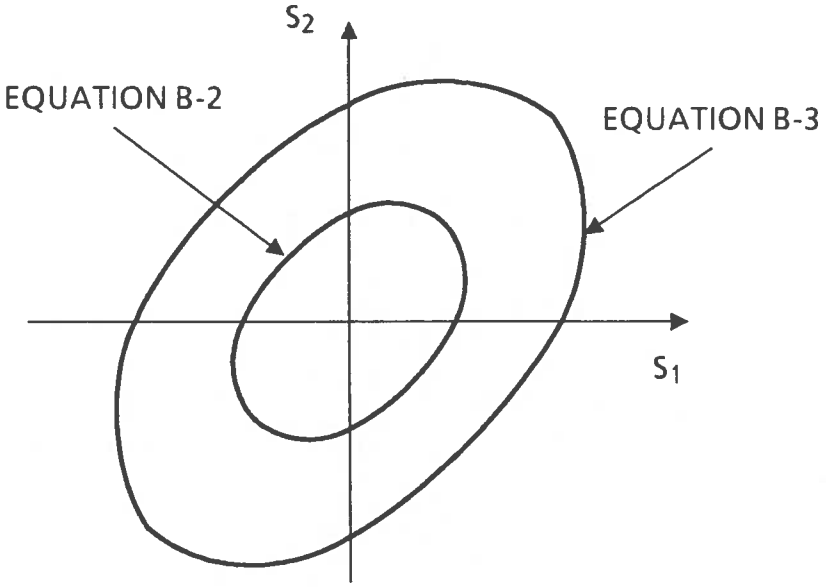

FIGURE B-2. MISES-HENCKY YIELD CRITERION

The tank shell bursting pressure can now be calculated by substituting the expressions for pressure stress in Equation B-3. The result,

$$P = \frac{4S_U t}{D\sqrt{3}} \tag{B-4}$$

is greater than the conventional burst pressure:

$$P = \frac{2S_U t}{D} \tag{B-5}$$

which is calculated from the hoop stress alone, i.e., $S_2 = S_U$ instead of Equation B-3. Equation B-5 is the proper calculation for design because the entire shell must be considered, and some stress concentration may persist up to the burst point at major attachments.

It is reasonable to use Equation B-4 for the present analysis, however, since there are no major structural discontinuities near the former bracket locations where ground areas are to be found. The equation is applied by replacing t with $t_{nom} - d$, where t_{nom} is the nominal wall thickness and d is the defect depth.

The foregoing analysis can also be applied to a fatigue crack defect. Under the assumed condition of fire engulfment, the shell's high temperature makes the material sufficiently ductile to blunt the crack tip during slow loading by the increasing internal pressure. In this case, the defect depth d is the critical crack size that defines the end of fatigue crack growth life (see Appendix A).

There is no general standard for tank car bursting strength under the conditions of fire engulfment. The only specific standard (49 CFR 179.105-4, 1984) requires that DOT-112T, -112J, -114T, and -114J cars be able to survive a 100-minute pool fire and a 30-minute torch fire without release of the car's contents (except through the safety valve). Under the present circumstances, it appears reasonable to apply the pool fire criterion to the affected fleet. The wall temperature and internal pressure at 100 minutes then determine the depth of a defect that will allow the tank to burst at the pool fire time limit. (The wall temperature affects the shell strength.)

The temperature and pressure depend on the the flow capacity of the relief valve and the orientation of the car. Design capacities of tank car relief valves vary from about 300 to nearly 30,000 cubic feet per minute at standard conditions (SCFM), with 3,000 SCFM being a representative capacity for the affected fleet. The worst orientation, based on accident experience, is a 120-degree overturn. A car in this orientation will expose the shell wall to dry conditions (and high temperatures) when about 75 percent of the tank volume is still filled with liquid (Figure B-3). The flow capacity is also diminished because the valve must release liquid, and the internal pressure is correspondingly increased.

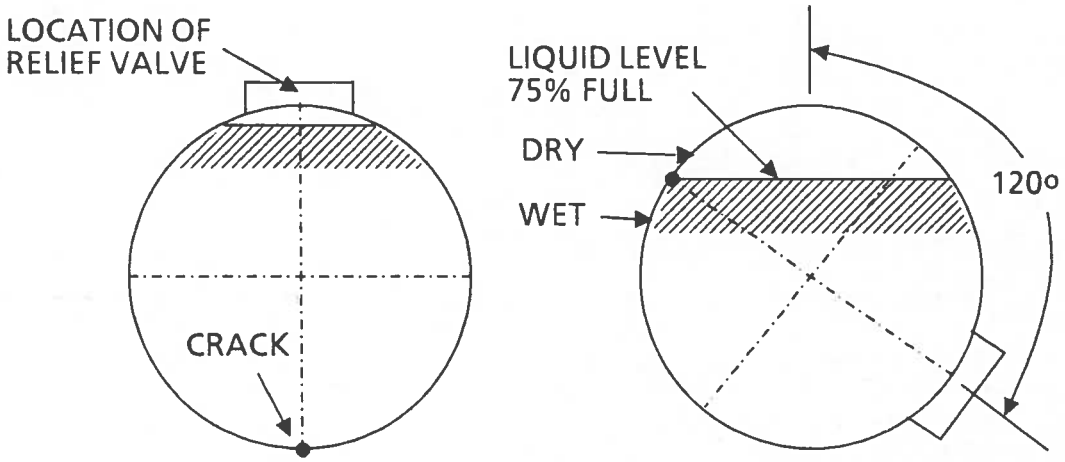

(A) UPRIGHT (B) OVERTURNED

FIGURE B-3. CAR ORIENTATION

The temperature and pressure also depend on the conductance of the car's exterior insulating jacket and the thermal properties of the commodity being carried. Higher conductance (less insulation) means higher heat input rate and, therefore, less time to reach a given temperature or pressure. In a similar manner, less time is required for a

commodity with lower heat capacity, heat of vaporization, and/or lower boiling point to reach a given temperature or pressure.

The transient temperature-pressure-time history for an overturned car engulfed in a pool fire can only be obtained by means of experiment or detailed simulation. Some full scale experiments have been performed on tank cars containing water, and the results of these tests have been used to develop calculation procedures for simulation of pool fire effects on cars containing hazardous commodities (Johnson, 1984). Table B-1 summarizes the available simulation results for seven commodities assumed to be carried in cars with 9/16-inch walls and 3,000 to 3,070 SCFM relief valves. Six of the seven simulations suggest that the nominal (undamaged) car can sustain significantly higher pressure and/or temperature, before failing, than the pressure and temperature at the 100-minute point. Hence, a car with a defect deep enough to fail under the 100-minute conditions poses a greater risk than the nominal car.

TABLE B-1. SIMULATION RESULTS

Commodity	Conductance (Btu/hrft^{2}oF)	Conditions at 100 minutes		Conditions at calculated failure	
		P (psig)	T (oF)	P (psig)	T (oF)
Propylene	3.0	550	700	856	710
Propane	3.0	400	725	624	750
1,3 Butadiene	5.4	260	875	350	875
Vinyl chloride	4.0	300	800	396	810
Monomethylamine	5.4	220	850	532	880
Ethylene oxide	5.4	150	850	62	1400
Propylene oxide‡	5.4	60	885	61	900

‡Result interpolated from simulations with 1,100 and 5,000 SCFM relief valves.

The simulation uses a reduced material ultimate strength versus temperature to calculate the failure point based on the dry, hot wall section. Figure B-4 illustrates the strength-temperature curve reconstructed from the simulation results. The curve is presented in terms of the nondimensional strength factor:

$$F_S = \frac{S_U(T)}{S_U} \tag{B-6}$$

where $S_U(T)$ is the strength at elevated temperature T. Also shown in the figure are steel strength data from two independent sources and a straight line that fits the data. The straight-line relation was used in the present calculations.

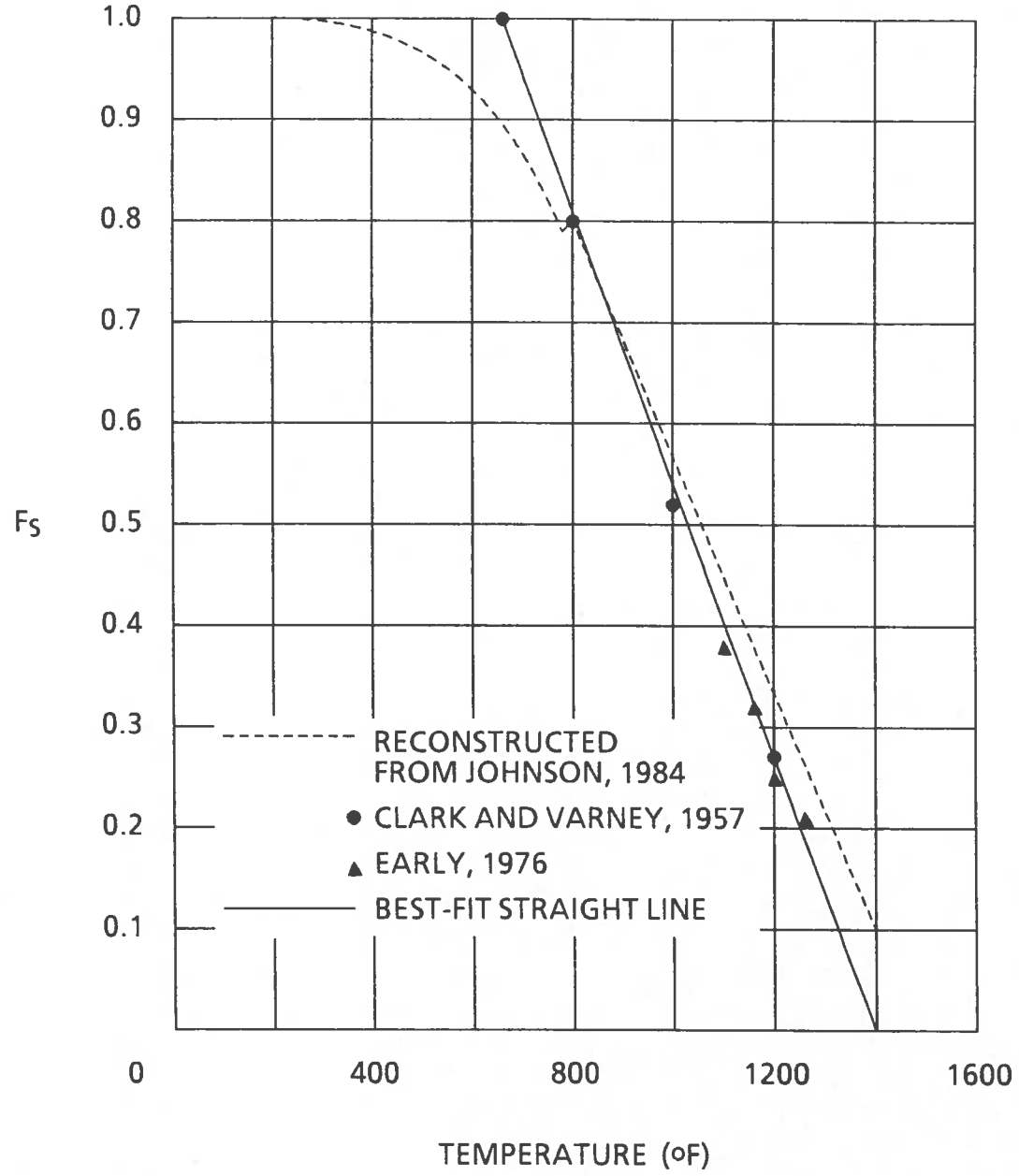

FIGURE B-4. STEEL STRENGTH VERSUS TEMPERATURE

For each of the cases in Table B-1, the net wall thickness $t = t_{nom} - d$ was calculated by substituting P and S_U (T) for the 100-minute conditions in Eq. B-4. Table B-2 summarizes the results and also shows the governing (minimum) defect depths for each nominal wall thickness. These results are based on A515 Grade 70 steel, which has lower strength than TC128 and which is the most prevalent material in the affected fleet.

The smallest defect depths are obtained from the case of propylene, a liquefied flammable gas. This case does not apply to the 7/16-inch wall, which is found only in DOT-111A/100W cars; current regulations (49 CFR 179, 1984) forbid these cars from carrying liquefied flammable gases. The defect depth calculated for the 9/16-inch wall

is less than the initial crack depth assumed in Appendix A; this suggests that the risk of carrying propylene in affected cars with 9/16-inch walls is not acceptable. The propylene case does determine the critical defect depth for cars with 11/16-inch walls.

The second smallest defect depths are obtained from the case of propane, another liquefied flammable gas. This case determines the critical defect depth for cars with 9/16-inch walls.

Of the seven commodities which were assumed in the simulations, only ethylene oxide and propylene oxide are permitted in DOT-111A/100W cars (49 CFR 179, 1984), and the ethylene oxide case gives the smaller of the two defect depths. Therefore, this case is used to determine the critical defect depth for cars with 7/16-inch walls.

TABLE B-2. CRITICAL DEFECT DEPTHS

Commodity	$t = t_{nom} - d$ (in.)	Defect depth (in.) for 7/16 wall	Defect depth (in.) for 9/16 wall	Defect depth (in.) for 11/16 wall
Propylene	0.410		0.152	0.277
Propane	0.308		0.254	
1,3 Butadiene	0.261			
Vinyl chloride	0.260			
Monomethylamine	0.209			
Ethylene oxide	0.142	0.295		
Propylene oxide	0.063			

Appendix C - Confidence Levels for Small Sample Inspections

If the affected fleet still has a small percentage of cars with defects, and if another small percentage is chosen at random for inspection, there is a chance that the inspected cars will include some of the defective cars. This chance increases as the percentage of defective cars increases and as the inspection sample size increases (Figure C-1). For given defect rate and sample size, the confidence level of the inspection can be defined as the probability that the sample includes at least one defective car. The confidence level can be calculated from standard probability distribution formulas (Wadsworth and Bryan, 1960).

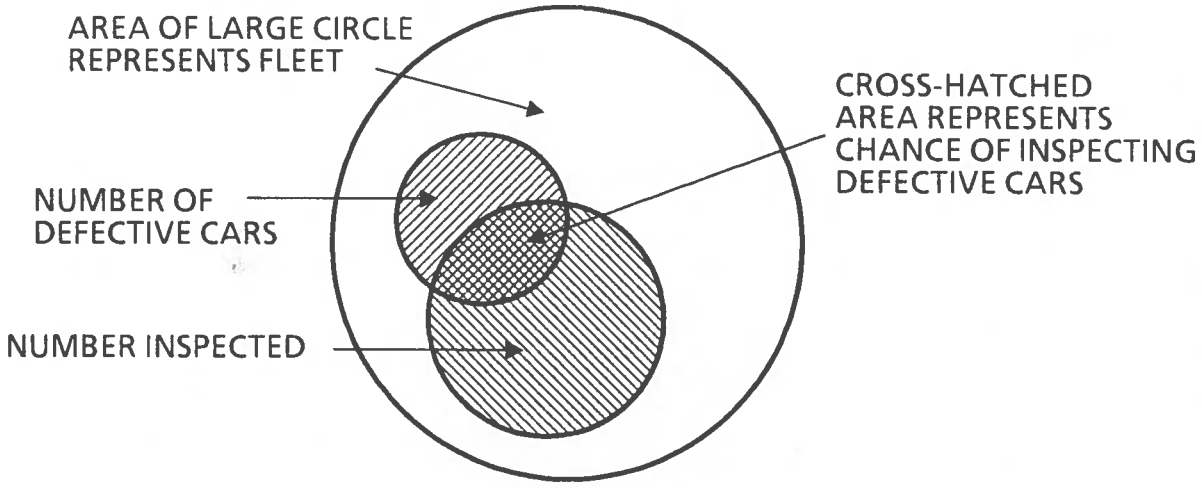

FIGURE C-1. PROBABILITY DIAGRAM FOR SMALL-SAMPLE INSPECTION

Let N be the number of cars in the fleet, m be the number of defective cars, n be the number inspected. Then the probability $P(x)$ that the sample n includes exactly x ($<m$) defective cars is given by the hypergeometric distribution,

$$P(x) = \frac{C(m,x)\,C(N-m,n-x)}{C(N,n)} \qquad \text{(C-1)}$$

where $C(p,q)$ is the binomial coefficient:

$$C(p,q) = \frac{p!}{q!\,(p-q)!} \qquad \text{(C-2)}$$

If $x \ll m$ and m and n are small compared to N, then the hypergeometric distribution can be approximated by the binomial distribution, and the probability of exactly x defective cars in the sample becomes:

$$P(x) = C(n,x)\left[\frac{m}{N}\right]^{x}\left[1-\frac{m}{N}\right]^{n-x} \qquad \text{(C-3)}$$

In particular, the probability that the sample includes no defective cars is given by:

$$P(0) = [\,1 - \frac{m}{N}\,]^n = 1 - c \qquad \text{(C-4)}$$

where c is the desired confidence level. Equation C-4 can be further simplified by taking the natural logarithm,

$$n\ \ell n[\,1 - \frac{m}{N}\,] = \ell n(1-c) \qquad \text{(C-5)}$$

and noting that:

$$\ell n[\,1 - \frac{m}{N}\,] \simeq \frac{m}{N}\,[\,1 + \frac{m}{2N}\,] \qquad \text{(C-6)}$$

for small m/N. Substituting Eq. C-6 in Eq. C-5 then gives the following formula for the sample size in terms of the confidence level c and the fleet defect rate m/N:

$$n \simeq \frac{-\ell n(1-c)}{\frac{m}{N}\,[\,1 + \frac{m}{2N}\,]} \qquad \text{(C-7)}$$

A 90 or 95 percent confidence level ($c = 0.9$ or 0.95) is consistent with accepted statistical practice and the level of risk involved in the present case. Figure C-2 shows how the inspection sample size depends on the fleet defect rate for these confidence levels. These results can be applied by recalling that the manufacturer's initial inspection found 200 defective cars out of the first 3,000 inspected. Although over 7,400 cars had been inspected by mid-December 1985, no additional data on defective cars has been received. Since the sample size required for a given confidence increases as the defect rate decreases, it is conservative to assume that the demonstrated defect rate is 200 out of 9,000 cars, or about 2 percent, and to establish as the sample inspection goal the confident detection of a similar defect rate, if such exists, after the fleet has been returned to service. Therefore, the results in Figure C-2 suggest that the appropriate sample size is 150 cars.

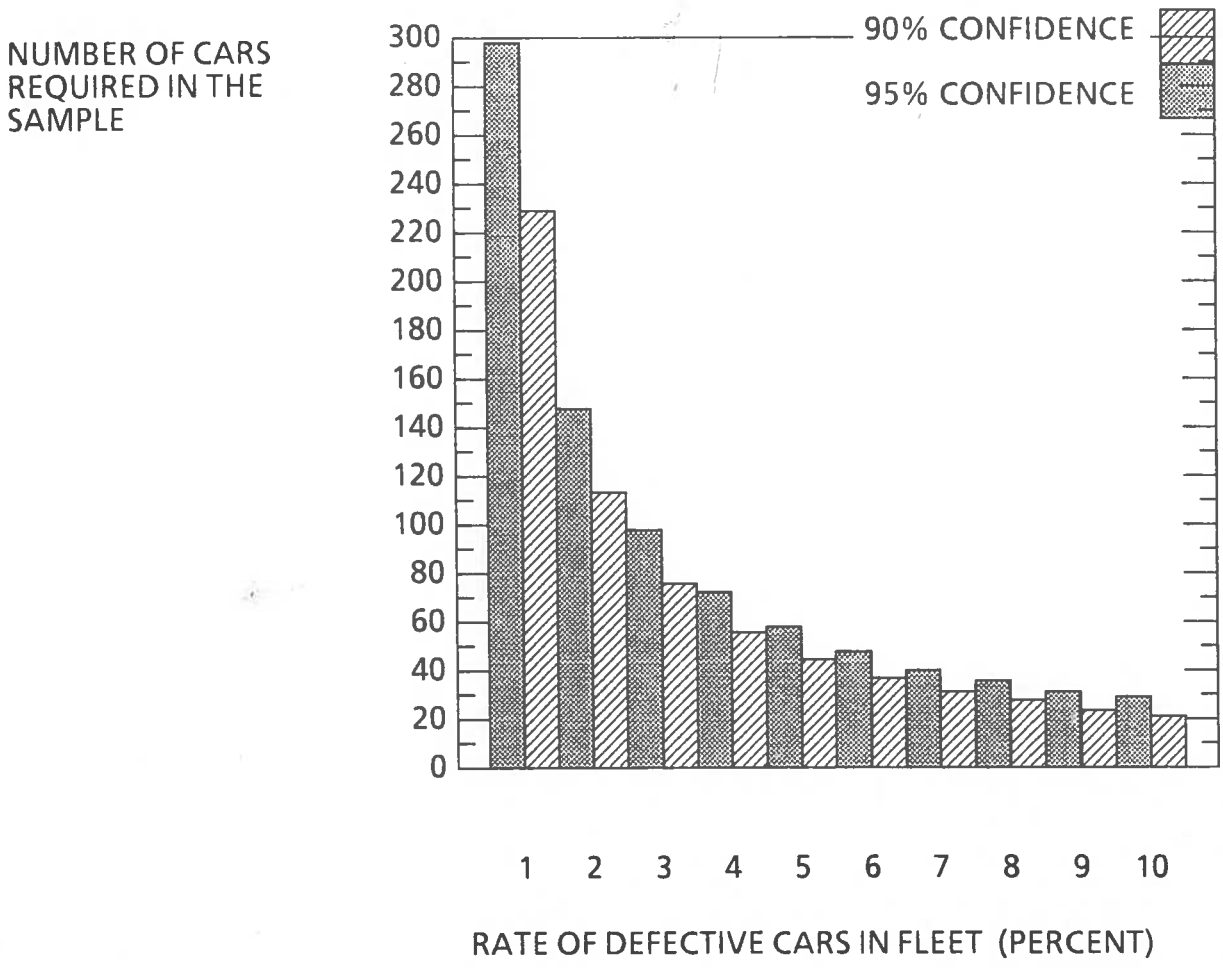

FIGURE C-2. INSPECTION SAMPLE SIZE VERSUS DEFECT RATE

Appendix D - Bibliography

Anon., ASME Pressure Vessel and Boiler Code, Section IX, Part QW Welding, American Society of Mechanical Engineers, ANSI/ASME BPV-IX, 1977.

Anon., "Manual of Standards and Recommended Practices - Specifications for Tank Cars," Association of American Railroads, Washington, DC, Standard M-1002, January 1982 (Rev. January 1983).

Anon., "Damage Tolerance and Fatigue Evaluation of Structure", Federal Aviation Administration, Washington, DC, AC 25.571-1, September 1978.

Anon.' "Standard Practice for Liquid Penetrant Inspection Method", American Society for Testing and Materials, Philadelphia, PA, ASTM Standard E165-80 (1983).

Anon., "Railcar Maintenance Instruction - Engineering Instructions," General American Transportation Corporation, Chicago, IL, No. FM-1147 Rev. E, June 11, 1985; Rev. H, August 30, 1985.

J. Burnett, P.A. Goldman, and G.H.P. Bursley, "Hazardous Materials Special Investigation Report – Hazardous Materials Release; Missouri Pacific Railroad Company's North Little Rock, Arkansas, Railroad Yard, December 31, 1984", National Transportation Safety Board, Washington, DC, September 4, 1985.

J.E. Campbell et al., "Damage Tolerant Design Handbook", Materials and Ceramics Information Center, Battelle Columbus Laboratories, Columbus, Ohio, MCIC-HB-01, 1975.

D.S. Clark and W.R. Varney, Physical Metallurgy for Engineers, D. Van Nostrand Company, Inc., Princeton, NJ, 5th ed., 1957.

Code of Federal Regulations, Title 14, "Aeronautics and Space", Part 25, "Airworthiness Standards: Transport Category Airplanes", January 1984.

Code of Federal Regulations, Title 49, "Transportation", Part 179, "Specifications for Tank Cars", November 1984.

C.L. Combes (ed.), Car and Locomotive Cyclopedia, Simmons-Boardman Publishing Corporation, New York, 1970, pp. 248-249.

J.G. Early, "Mechanical Properties of AAR M128-69-B Steel Plate Samples Taken from Insulated Fire Tested Tank Car", National Bureau of Standards, Washington, DC, Report No. FRA/OR&D 76-74, June 1976.

F. Erdogan, "Theoretical and Experimental Study of Fracture in Pipelines Containing Circumferential Flaws", Department of Mechanical Engineering and Mechanics, Lehigh University, Bethlehem, PA, Report No. DOT-RSPA-DMA-50/83/3, August 1982.

C.G. Interrante, "Impact Properties of Steels Taken from Four Failed Tank Cars", National Bureau of Standards, Gaithersburg, MD, Report No. FRA-OR&D 75-51, June 1976.

M.R. Johnson, "Summarization and Comparison of Freight Car Truck Load Data", ASME Transactions, Journal of Engineering for Industry, Vol. 100 (February 1978), pp. 60-66.

M.R. Johnson, "Temperatures, Pressures and Liquid Levels of Tank Cars Engulfed in Fires - Volume 1, Results of Parametric Analysis", IIT Research Institute, Chicago, IL, Report No. DOT/FRA/OR&D-84-08, June 1984.

W.H. Lewis et al., "Reliability of Nondestructive Inspections", Lockheed Georgia Company, Marietta, GA, final report to USAF San Antonio Air Logistics Center, Kelly AFB, TX, SA-ALC/MME 76-6-38-1, 1978.

L.E. Marsh et al., "Liquid-Penetrant Inspection", in Metals Handbook, Vol. 11, Nondestructive Inspection and Quality Control (H.E. Boyer, ed.), American Society for Metals, Metals Park, OH, 8th ed., 1976.

F.A. McClintock and A.S. Argon, Mechanical Behavior of Materials, Addison-Wesley Publishing Company, Reading, MA, 1966.

Military Specification, "Airplane Damage Tolerance Requirements", MIL-A-83444 (USAF), 1972.

E. Mowatt-Larssen, General American Transportation Corporation, Chicago, IL, letter to J.W. Walsh, Associate Administrator for Safety, FRA, July 11, 1985.

O. Orringer and P. Tong, "Results and Analysis of the Switchyard Impact Tests", DOT Transportation Systems Center, Cambridge, MA, Report No. DOT-TSC-FRA/ORD-80/6, January 1980.

O. Orringer, "Rapid Estimation of Spectrum Crack Growth Life Based on the Palmgren-Miner Rule", Computers & Structures, Vol. 19 No. 1-2 (1984a), pp. 149-153.

O. Orringer, "Failure Mechanics: Damage Evaluation of Structural Components", in Fracture Mechanics Methodology: Evaluation of Structural Components Integrity (G.C. Sih and L. Faria, ed.), Martinus Nijhoff Publishers, the Hague, the Netherlands, 1984b.

O. Orringer and P. Tong, "Structural Integrity Assessment of the Flxible 870 Advanced Design Bus", in Fracture Problems in the Transportation Industry (P. Tong and O. Orringer, ed.), Proceeding of the Engineering Mechanics Division, American Society of Civil Engineers, Detroit, MI, October 1985.

P.F. Packman et al., "Definition of Fatigue Cracks Through Nondestructive Testing", Journal of Materials, Vol. 4, No. 3 (September 1969), pp. 666-700.

W.S. Pellini, "Feasibility Analysis for Tank Car Applications of New Microalloyed and Controlled Rolled Steels - Description of Fracture Properties and Comparisons with Steels in Present Use", Research and Technical Center, Association of American Railroads Chicago, IL, Report No. R-543, April 1983.

S.T. Rolfe and J.M. Barsom, Fatigue and Fracture Control in Structures, Prentice-Hall, Englewood Cliffs, NJ, 1977.

H.H. Uhlig, Corrosion and Corrosion Control, Wiley, New York, 2nd ed., 1971.

G.P. Wadsworth and J.G. Bryan, Introduction to Probability and Random Variables, McGraw-Hill, New York, 1960.

Appendix E - Task Force Composition

Dr. Pin Tong (Chairman)

Dr. Tong received his PhD degree in aeronautical mathematics from the California Institute of Technology in 1966. He has twenty years of experience in the analysis and design of mechanical systems. During the past eight years at the Transportation Systems Center, he has been responsible for directing and conducting analytical and experimental studies and designing mechanical components of transportation vehicles and systems. He is the author of numerous original papers on structural analysis and a book on the finite element method. He is a 1974 recipient of the Von Karman Award for outstanding contributions to the field of solid mechanics.

Dr. Fazil Erdogan

Dr. Erdogan received his PhD degree from Lehigh University in 1955. He is professor and chairman of the Department of Mechanical Engineering and Mechanics, Lehigh University. He is a nationally recognized authority on the mechanics of fracture and has published numerous original papers on mathematical methods for analysis of fracture instability under plasticity conditions. His work has included assessment of gas transmission pipeline fracture criteria for the DOT. He is a 1983 recipient of the Alexander von Humboldt Senior U.S. Scientist Award.

Dr. Richard Fields

Dr. Fields received his PhD in engineering from Cambridge University, England, in 1977. He joined the National Bureau of Standards after receiving his degree. He is presently a group leader in the Fracture and Deformation Division. He has numerous publications in the area of fracture mechanics and also serves on several ASTM committees.

Dr. Frank A. McClintock

Dr. McClintock received his PhD degree in mechanics of materials from the California Institute of Technology in 1949. He has been a member of the MIT faculty from 1949 to the present, becoming a full professor in 1959. He is a nationally recognized authority on fracture mechanics and the mechanics of incremental plasticity. He has published numerous original papers in these fields and a book on mechanics of materials. He is a registered professional engineer and a fellow of the American Academy of Arts and Sciences. He is a 1978 recipient of the Nadai Medal of the American Society of Mechanical Engineers for his research in materials science.

Dr. Oscar Orringer

Dr. Orringer received his ScD degree in structural mechanics from the MIT Department of Aeronautics and Astronautics in 1972. He leads the Transportation Systems Center's work on failure investigations involving fatigue and other mechanical or structural failures in transportation vehicles or structures. Prior to his entry into government service in 1978, he was a member of the MIT research and academic staffs. He was also a special advisor to the USAF Aeronautical Systems Division, where he participated in structural integrity assessments of the C-5A, C/KC-135, and F-4E/F aircraft fleets.

Dr. Regis M. Pelloux

Dr. Pelloux received his ScD degree from the MIT Department of Metallurgy in 1958, and has been a professor of materials science and engineering at MIT since 1968. He has ten years of professional experience in metallurgy and applied fracture mechanics as a research engineer and scientist for the Boeing Company. He is a nationally recognized authority in fracture mechanics and failure analysis and is often sought internationally for his technical opinion on structural failures. He is the author of numerous original papers on the metallurgy of fatigue crack growth and fracture. He

is a fellow of the American Society of Metals (ASM) and a 1968 recipient of the ASM Lucas Metallographic Award.

Dr. A. Benjamin Perlman

Dr. Perlman received his PhD degree in mechanics from Lehigh University in 1965. He is a professor of mechaical engineering at Tufts University. He has worked closely for several years as a visiting scholar with the Transportation Systems Center. His work at the Center has focussed on the mechanical and structural performance of rails and railroad vehicles.

Dr. George C.M. Sih

Dr. Sih received his PhD degree in mechanics from Lehigh University in 1960. He joined the Lehigh faculty in 1960 and was promoted to full professor in 1965. He is also the director of Lehigh's Institute of Fracture and Solid Mechanics. He has been principal investigator for over sixty engineering mechanics projects for the Office of Naval Research, Naval Research Laboratory, National Aeronautics and Space Administration, U.S. Air Force, U.S. Army, and other government agencies. He is a member of the National Materials Advisory Board, the Ship Materials Fabrication and Inspection Committee, and national committees on nuclear reactor component integrity. He is the author of numerous original papers and three books on the mechanics of fracture. He is a 1975 recipient of the national achievement award from the Chinese Institute of Engineers in the U.S.

Task force support staff

The task force was supported by four members of the Transportation Systems Center's technical staff. Mr. Michael R. Coltman received his MS degree from Tufts University in 1977, joined the Center in 1978, and is responsible for research on rail vehicle dynamic response, rail lateral restraint, and tank car crashworthiness. Mr. Jeffrey Gordon received hid BS degree from Tufts University in 1984, joined the Center in 1984, and recently completed a key technical staff assignment on a general aviation aircraft structural integrity assessment. Mr. James M. Morris holds a MS degree in physics from Boston College and has over twenty years experience in metallurgy; he has been with the Center for over ten years, during which he has worked primarily in the area of rail and railroad wheel metallurgy. Mr. David Y. Jeong received his MS degree in mechanical engineering from Tufts University in 1980 and joined the Center in 1980; his recent experience includes fatigue loads and crack growth assessment for rails in typical freight service environments